geosciences

MDPI

Review

Variety and Distribution of Diatom-Based Sea Ice Proxies in Antarctic Marine Sediments of the Past 2000 Years

Claire S. Allen [1,*] and Zelna C. Weich [1,2]

[1] British Antarctic Survey, High Cross, Madingley Road, Cambridge CB3 0ET, UK; zelch86@bas.ac.uk
[2] School of Earth and Environmental Sciences, Cardiff University, Main Building, Park Place, Cardiff CF10 3AT, UK
* Correspondence: csall@bas.ac.uk

Abstract: Antarctic sea ice is an essential component of the global climate system. Reconstructions of Antarctic sea ice from marine sediment cores are a vital resource to improve the representation of Antarctic sea ice in climate models and to better understand natural variability in sea ice over centennial and sub-centennial timescales. The Thomas et al. (2019) review of Antarctic sea ice reconstructions from ice and marine cores highlighted the prominence of diatom-based proxies in this research. Here, focusing solely on the diatom-based proxy records in marine sediments, we review the composition of proxies, their advantages and limitations, as well as the spatial and temporal cover of the records over the past 2 ka in order to assess the scope for future assimilation and standardization. The archive comprises 112 records from 68 marine cores, with proxies based on more than 30 different combinations of diatom taxa as well as the relatively new, highly branched isoprenoid (HBI) biomarkers.

Keywords: sea ice; Antarctica; late Holocene; marine sediments; diatoms; Southern Ocean

Citation: Allen, C.S.; Weich, Z.C. Variety and Distribution of Diatom-Based Sea Ice Proxies in Antarctic Marine Sediments of the Past 2000 Years. *Geosciences* **2022**, *12*, 282. https://doi.org/10.3390/geosciences12080282

Academic Editors: Jesus Martinez-Frias and Juan Pablo Corella

Received: 13 June 2022
Accepted: 8 July 2022
Published: 22 July 2022

1. Introduction

The annual growth and retreat of sea ice is one of the most dramatic and dynamic seasonal patterns on Earth today. In the Southern Ocean, the seasonal expansion of sea ice effectively doubles the surface area of Antarctica and exerts a powerful influence over global climatic, oceanographic, and biological systems. Satellite observations provide detailed records of sea ice cover over the past 40 years and highlight the inter-annual variability in sea ice distribution [1]. Since 1979, whilst the Arctic region has seen a pronounced decline in sea ice cover, the total area of Antarctic sea ice has gradually increased, interrupted only with a precipitous decline between 2014 and 2017, resulting in an overall modest expansion [2]. The trend in the total area of Antarctic sea ice masks substantial inter-annual variation and strong regional divergence (e.g., marked reduction (increase) in the Bellingshausen (Ross) Sea [3]), contradicting the decreasing trajectory of sea ice cover predicted by the majority of climate simulations [2,4–6]. An improved understanding of the influence and response of Antarctic sea ice to climate change is of primary importance in order to improve the accuracy and predictive competence of climate models tasked with simulating future global change [7].

To resolve pre-satellite trends in sea ice cover and put recent changes into the context of natural variability, longer archives are needed to resolve decadal-to-centennial variations and establish the pre-industrial state of Antarctic sea ice. Thomas et al. [8] show that the majority of Antarctic sea ice reconstructions for the past 2 ka from marine sediment cores are derived from "diatom proxies". Diatoms inhabit a diverse range of habitats within the Southern Ocean and its sea ice; individual species have unique requirements for light, temperature, salinity, and nutrient availability, and may bloom at different points in the year (Appendix A). The ecological preferences of these diatoms allow their fossils to be used as proxies for environmental changes. Biomarkers from a range of primary producers

preserved in the sedimentary record have been used to investigate past environmental changes [9]. Over the past 10 years, biomarkers specific to diatoms have been developed as a sea ice proxy. The di-unsaturated C_{25} highly branched isoprenoid (HBI) alkene (known as diene or HBI-II) and the tri-unsaturated C_{25} HBI alkene (known as triene or HBI-III) are produced by a small number of Southern Ocean diatom species and are preserved in marine sediments [10]. The source-specific nature of these biomarkers allow for their use as effective proxies.

Diatom proxies are typically considered more robust than other proxies as they provide a direct link between the sea ice environment and the sediment archive. However, there is great variety in the composition and approaches grouped within the "diatom proxies". This diversity reflects the wide range of oceanographic settings of the core sites and the sensitivity of diatom assemblages to environmental gradients. Providing a detailed review of the proxies and the most commonly employed taxa, followed by mapping out the distribution and resolution of existing records, will readily show areas where regional syntheses may be possible; highlight gaps in the existing coverage of sea ice records; and provide valuable information on the suitability, application, and comparison of diatom-based proxies for different regions of Antarctica.

The structure of the paper is as follows:

- In the first section, we collate all the published marine sediment records spanning all, or part, of the past 2000 years with sea ice reconstructions derived from diatom-based proxies. We review the composition and variety of proxies used to reconstruct sea ice and map their distribution.
- We then consider the advantages and limitations of the proxies and discuss the potential for improving consistency/standardization between records and the scope for regional syntheses.

2. Results

In order to maximize the number of records included in this study, broad selection criteria were adopted: (1) include at least two data points to infer sea ice conditions during some or all of the past 2 ka, (2) a dated horizon to establish the surface/near-surface age (e.g., lead-210; radiocarbon) and at least one other dated horizon to determine the depth of the 2 ka interval. Records that were published up to and including 2021 were all considered, but duplicated records with matching age models and resolution were excluded. These criteria were met by 112 proxy records from 68 marine core sites, comprising 8 sites from the deep Southern Ocean and 60 from the Antarctic continental shelf (Figure 1 and Table 1 [11–68]). Duplicate and lower resolution records in other publications were also excluded. All dates were based on the published age models and presented in the same units as in the original publications. Radiocarbon dates were reported as either corrected radiocarbon (^{14}C ka BP) or calendar (ka BP) ages. The mean offset between calendar and ^{14}C ages for the 2 ka time interval is +/−0.092 ka [69].

Table 1. Marine core sites with diatom-based sea ice proxy records for all or part of the past 2 ka.

Map Ref.	Core/Site ID	Lat	Long	Location Name	References
1	WG35	−77.989	162.853	Granite Harbor, Western Ross Sea	[11]
2	Multiple	−77.668	165.500	McMurdo Sound; Western Ross Sea	[12]
3	WG17	−77.000	162.850	Granite Harbor, Western Ross Sea	[11]
4	KC208.09	−76.972	162.876	Granite Harbor, Western Ross Sea	[11]
5	KC31	−75.700	165.418	Western Ross Sea	[13]
6	KC37	−74.499	167.744	Western Ross Sea	[13]
7	KC39	−74.474	173.474	Western Ross Sea	[13]
8	BAY05-43c	−74.000	166.050	Wood Bay, Western Ross Sea	[14]
9	ANTA99-cJ5	−73.817	175.650	Joides Basin, Western Ross Sea	[14]
10	KC17	−73.420	−102.827	Ferrero Bay, Amundsen Sea Embayment	[15]
11	KC15	−73.360	−101.836	Ferrero Bay, Amundsen Sea Embayment	[15]

Table 1. *Cont.*

Map Ref.	Core/Site ID	Lat	Long	Location Name	References
12	BAY05-20c	−72.300	170.050	Cape Hallet, Ross Sea	[14]
13	AM02	−69.713	72.640	Amery Ice Shelf, Prydz Bay	[16]
14	CO1011	−68.827	77.760	Flag Island Inlet, Prydz Bay	[17]
15	CO1010	−68.817	77.833	Filla Island Inlet, Prydz Bay	[17]
16	JPC24	−68.694	76.709	Svenner Channel, Prydz Bay	[18–20]
17	KROCK-15-GC29	−68.664	76.696	Prydz Bay	[21]
18	Abel Bay	−68.650	78.400	Long Fjord, Ingrid Christensen Coast	[22]
19	Watts Basin	−68.603	78.213	Ellis Fjord, Ingrid Christensen Coast	[23]
20	Deep Basin	−68.560	78.199	Ellis Fjord, Ingrid Christensen Coast	[23]
21	Platcha Bay	−68.515	78.478	Long Fjord, Ingrid Christensen Coast	[22]
22	JPC43	−68.257	−66.962	Neny Fjord, Marguerite Bay, AP	[24]
23	TPC522	−67.856	−68.205	Marguerite Bay, AP	[25]
24	KROCK-125-GC2	−67.474	64.973	Nielsen Bay, MacRobertson Land	[26]
25	GC1	−67.180	−66.797	Lallemand Fjord, AP	[27]
26	JPC41	−67.131	62.990	Iceberg Alley, MacRobertson Land	[28]
27	GC 5	−67.059	69.016	MacRobertson Shelf, Prydz Bay	[29]
28	KROCK-128-GC1	−66.983	63.154	Iceberg Alley, MacRobertson Land	[26]
29	CB2010	−66.906	142.436	Commonwealth Bay, Adélie Land	[30]
30	PG1433	−66.465	110.572	Browning Bay, Windmill Is., Wilkes Land	[31]
31	PG1430	−66.453	110.498	Peterson Inlet, Windmill Is., Wilkes Land	[31]
32	MD03-2597	−66.412	140.421	Dumont d'Urville Trough, Adélie Land	[32]
33	DTCI2010; 318-1357B	−66.411	140.445	Dumont d'Urville Trough, Adélie Land	[33,34]
34	PG1173	−66.267	100.750	Bunger Oasis, Wilkes Land	[35]
35	MD03-2601	−66.052	138.557	Dumont d'Urville Trough, Adélie Land	[20,36–39]
36	WAP13-GC47	−65.613	−64.759	Bigo Bay, AP	[40]
37	JPC10/178-1098	−64.883	−64.200	Palmer Deep, AP	[41–43]
38	PD92-30	−64.862	−64.208	Palmer Deep, AP	[44,45]
39	TC46/GC47	−64.588	−64.805	Anvers Shelf, AP	[46]
40	MTC18A	−64.772	−62.829	Andvord Drift, Gerlache Strait, AP	[47]
41	GC 02	−64.000	−64.000	Anvers Shelf, AP	[48]
42	KC2B	−63.971	−57.759	Herbert Sound, James Ross Island, AP	[49]
43	MTC38C, JPC38	−63.717	−57.411	Vega Drift, Prince Gustav Channel, AP	[47,50]
44	PC61	−63.389	−60.319	Western Basin, Bransfield Strait, AP	[51]
45	JPC02	−63.343	−55.887	Firth Of Tay, Joinville Island, AP	[52]
46	A-3	−63.168	−59.302	Orleans Trough, Bransfield Strait, AP	[53,54]
47	JPC36	−63.089	−55.411	Perseverance Drift, Joinville Island, AP	[55]
48	GC 03	−63.000	−64.000	Anvers Shelf, AP	[48]
49	A-6	−62.912	−59.97	Western Basin, Bransfield Strait, AP	[53,54]
50	Gebra-1	−62.589	−58.542	Central Basin, Bransfield Strait, AP	[53,56]
51	1B	−62.282	−58.754	Maxwell Bay, South Shetland Is.	[57]
52	MC-01	−62.202	−58.727	Marian Cove, South Shetland Is.	[58]
53	WB2	−62.200	−60.700	Outer Shelf, South Shetland Is.	[59]
54	CB2	−62.191	−58.833	Collins Harbour, South Shetland Is.	[60]
55	Gebra-2	−61.943	−55.17	Eastern Basin, Bransfield Strait, AP	[53,56]
56	13PC (TN057-13PC4)	−53.200	5.1000	Atlantic-Indian Ridge, S Atlantic Ocean	[61]
57	E27-23	−59.618	155.238	Emerald Basin, SE Indian Ocean	[62]
58	PS1652-2	−53.664	5.100	Atlantic-Indian Ridge, S Atlantic Ocean	[63]
59	PS1768-8	−52.593	4.476	Atlantic-Indian Ridge, S Atlantic Ocean	[63]
60	177-1094/PS2090-1	−53.179	5.132	Atlantic-Indian Ridge, S Atlantic Ocean	[63,64]
61	PS2102-2	−53.073	4.986	Atlantic-Indian Ridge, S Atlantic Ocean	[63]
62	17PC (TN057-17PC1)	−50.000	6.000	Cape Basin, S Atlantic Ocean	[61]
63	COR1GC	−54.267	39.766	Conrad Rise, SW Indian Ocean	[65]
64	HLF17-1	−72.308	−172.054	Edisto Inlet, Ross Sea	[66]
65	PS97/056-1	−64.757	−60.442	Gilbert Strait, Bransfield Strait, AP	[67]
66	PS97/068-2	−63.168	−59.302	Orleands Trough, Bransfield Strait, AP	[67]
67	PS97/072-2	−62.007	−56.065	Eastern Basin, Bransfield Strait, AP	[67]
68	DTGC2011	−66.408	140.441	Dumont d'Urville Trough, Adélie Land	[68]

AP—Antarctic Peninsula

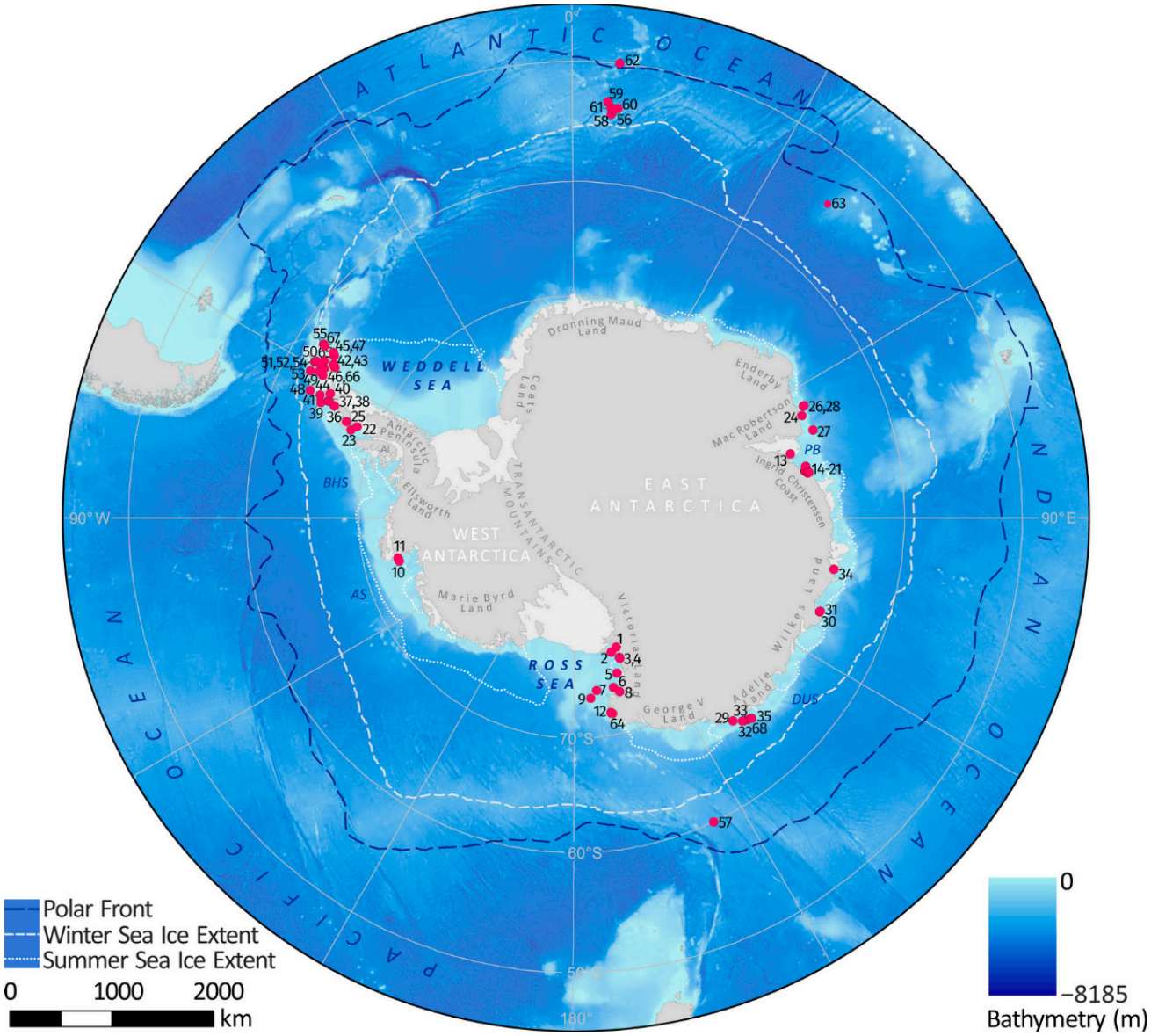

Figure 1. Map showing sites (red-filled circles) of published marine sediment core records with diatom-based sea ice proxies for all or part of the past 2 ka. Sites are numbered corresponding to the map references given in Table 1. AS—Amundsen Sea; BHS—Bellingshausen Sea; DUS—Dumont d'Urville Sea; PB—Prydz Bay. Winter and summer sea ice limits depict the 1981–2010 median September and February sea ice extents (Source: /DATASETS/NOAA/G02135/south/monthly/).

2.1. Proxy Records

The 112 records comprise more than 30 individually described diatom-based sea ice proxies across 68 marine sites. Of the 112 records, 30 are based on a single species, 16 on two species, 10 on transfer functions, 14 on diatom-specific HBI biomarkers and the remaining 42 are based on groups of more than two species.

Fragilariopsis curta is included in 77 of the 112 proxy records and is the most common diatom taxa used in reconstructions of Antarctic sea ice (Table 2). Of these 77 records, 23 are based solely on *F. curta*% and 54 comprising various groups or ratios that include *F. curta* (Table 3). *F. cylindrus* is the second most common taxa and is included in the composition of 54 proxies. *Thalassiosira antarctica*, *Fragilariopsis sublinearis*, *F. obliquecostata*, *F. vanheurckii*, *F. rhombica*, *F. kerguelensis*, *Actinocyclus actinochilus*, *Porosira glacialis*, *F. ritscheri* and *F. separanda*

are each included in at least 10 of the 112 proxy records (Table 2). The habitat preferences of these species are available in Appendix A.

Table 2. The most common diatom taxa in Antarctic sea ice proxies of the past 2 ka.

Diatom Species	n
Fragilariopsis curta	77
Fragilariopsis cylindrus	54
Thalassiosira antarctica	21
Fragilariopsis sublinearis	21
Fragilariopsis kerguelensis	19
Fragilariopsis obliquecostata	19
Fragilariopsis rhombica	16
Fragilariopsis ritscheri	14
Fragilariopsis vanheurckii	14
Actinocyclus actinochilus	12
Porosira glacialis	12
Fragilariopsis separanda	10

Table 3. Number of records for different proxy categories.

	Categories	n
1.	*F. curta* + *F. cylindrus* (*F. c* + *cy*) %	10
2.	*F. curta* %	23
3.	*F. c* + *cy*/*T. antarctica*	3
4.	*F. curta*/*F. kerguelensis*	4
5.	Groups including *F. curta*	36
6.	Groups excluding *F. curta*	7
7.	Other	15
8.	HBIs	14
	TOTAL	112

The selection of taxa comprising the various groups is mostly based on statistical and/or ecological associations, but seasonal timing within varved sediments is also used to determine the composition of some groups [32,38]. Statistical techniques used to define groups include the modern analogue technique (MAT), the Imbrie Kipp method (IKM), the generalized additive model (GAM) method, principal component analysis (PCA), and cluster analysis [26,27,38,61–63,70]. Most proxies are used to infer qualitative changes in seasonal sea ice cover, whilst the MAT and GAM methods produce a quantitative estimate of sea ice conditions (e.g., months per year of sea ice cover or sea ice concentrations). In nearshore locations and sites close to ice shelves, some taxa and/or taxa groups are associated with more niche sea ice conditions or types e.g., the fast ice index [22,23,26].

In order to review the prevalence and distribution of proxies used to reconstruct sea ice in the marine 2 ka records considered here, the proxies were divided into eight categories according to their composition. As *F. curta* was the most commonly used diatom (Table 2), the diatom groups used as sea ice proxies were classified based on whether they included *F. curta* or not (Table 3).

Categories 1 to 4 are based on the relative abundances of 1–2 diatom species or on ratios of 2–3 diatom species that are used by more than two authors; categories 5 and 6 include proxies based on groups of >3 taxa that either include or exclude *F. curta*, respectively; category 7 contains all other diatom proxies that do not fit in categories 1–6, most of which are presented in a single publication or by a specific author; and category 8 comprises all HBI diatom-specific biomarker records. Further details regarding the habitat preferences associated with the diatoms used in these proxy categories are provided in Appendix A.

2.1.1. *Fragilariopsis curta + F. cylindrus* %

Based on the diatom assemblage composition of sediment trap material and surface sediments in the Atlantic sector of the Southern Ocean, Gersonde and Zielinski [71] demonstrated a close correlation between the combined relative abundance of *F. curta* and *F. cylindrus* (*F. c + cy* %) and the distribution of Antarctic winter sea ice. This study determined that the relative abundances of *F. c + cy* > 3% can be applied as a proxy for areas south of the mean winter sea ice extent in the Southern Ocean.

The *F. c + cy* % proxy is used in 10 records from nine sites across the deep South Atlantic (Sites 58, 59, 60, and 61), Palmer Deep (Sites 37 and 38), and the Dumont d'Urville Trough (Sites 33, 35, and 68; Figure 2). Nine of the *F. c + cy* % records extend from 2.0 ka BP to between 1.0 and 0.1 ka BP with maximum sample intervals between 190 and 600 years at the deep ocean sites and between 180 and 4 years for the continental shelf sites (Table 4). The highest resolution *F. c + cy* % record, with sampling intervals of 4 years or less, is from core DTGC2011 (Site 68) in the Dumont D'Urville Trough and spans from 0.4 to ~0 ka BP [68].

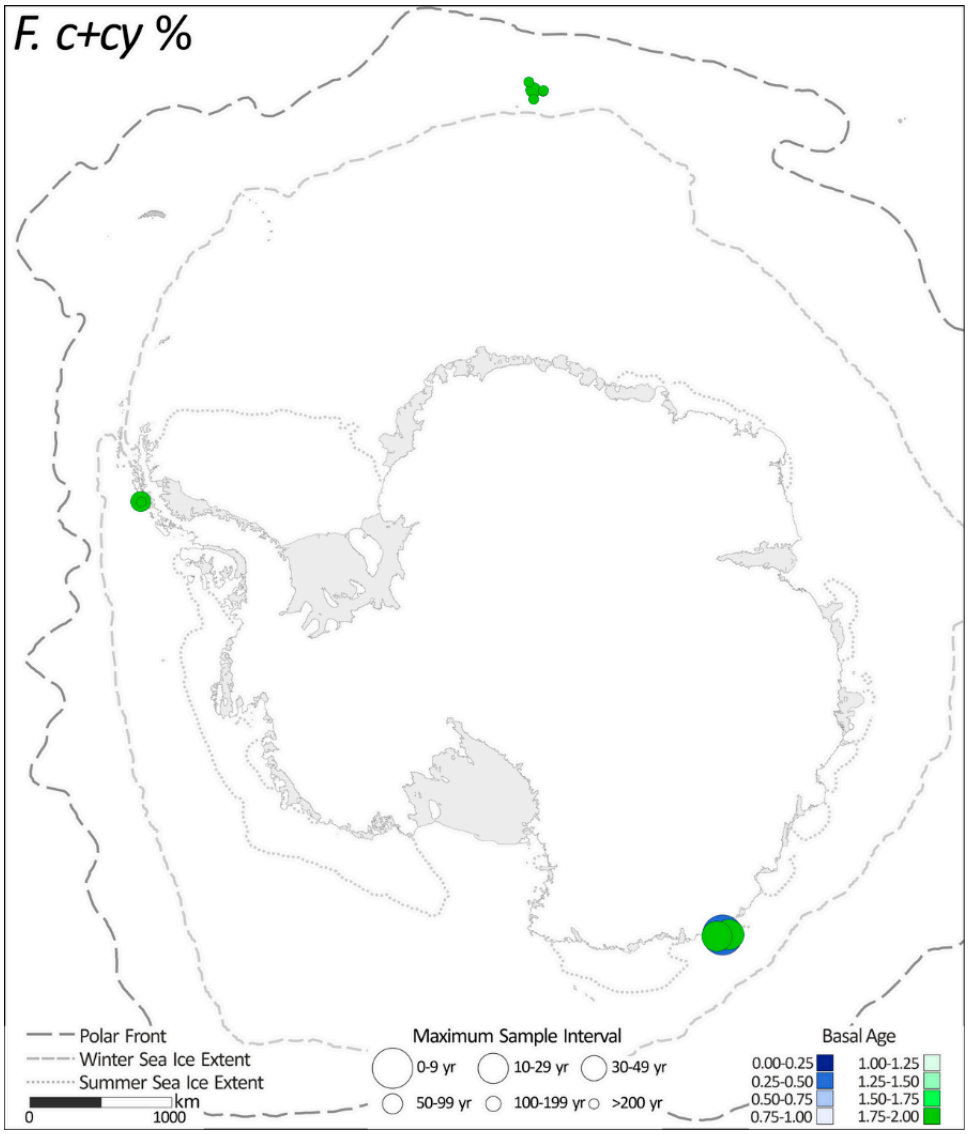

Figure 2. Map showing cores sites where *F. c + cy*% is used to reconstruct sea ice conditions. The symbol size reflects the resolution of the record and the color of the symbol indicates the basal age of the record between 0 and 2 ka BP.

Table 4. Summary information on the ages, resolution and proxy types of all sites.

Map Ref.	Core/Site ID	Approximate Dates *	Approx. SR (m/ka)	Resolution (Lowest) Δ	Resolution (Highest) Δ	Proxy Categories †	References
1	WG35	1.2 to ~0.6 ka BP	1.67	60	32	2	[11]
2	Multiple	0.5 to ~0 ka BP	1	100	56	2	[12]
3	WG17	1.2 to ~0.6 ka BP	1.17	60	32	2	[11]
4	KC208.09	1.3 to ~0 ka BP	2.46	65	33	2	[11]
5	KC31	2.0 to ~0 ^{14}C ka BP	0.19	400	222	2	[13]
6	KC37	2.0 to ~0 ^{14}C ka BP	0.11	400	222	2	[13]
7	KC39	2.0 to ~0 ^{14}C ka BP	0.33	400	222	2	[13]
8	BAY05-43c	2.0 to ~0.0 ka BP	2.13	38	15	2	[14]
9	ANTA99-cJ5	2.0 to ~1.0 ka BP	0.56	23	9	2	[14]
10	KC17	2.0 to ~0 ka BP	0.13	1000	500	7	[15]
11	KC15	2.0 to ~0 ka BP	0.13	1000	500	7	[15]
12	BAY05-20c	2.0 to ~0.1 ka BP	1.58	48	19	2	[14]
13	AM02	2.0 to ~0.0 ^{14}C ka BP	0.05	400	222	2	[16]
14	CO1011	2.0 to ~0 ka BP	0.6	1000, 1000	500, 500	5, 7	[17]
15	CO1010	2.0 to ~0 ka BP	2	400, 400	222, 222	5, 7	[17]
16	JPC24	2.0 to ~0.6 ka BP	1.43	70, 70, 70, 70	36, 36, 36, 36	5, 5, 7, 8	[18–20]
17	KROCK-15-GC29	2.0 to ~0 ^{14}C ka BP	0.13	400	222	5	[21]
18	Abel Bay	2.0 to ~0 ^{14}C ka BP	0.45	200, 200	51, 51	2, 6	[22]
19	Watts Basin	2.0 to ~0.2 ^{14}C ka BP	1.39	45	18	6	[23]
20	Deep Basin	2.0 to ~0.8 ^{14}C ka BP	2.42	30	12	6	[23]
21	Platcha Bay	2.0 to ~0.0 ^{14}C ka BP	0.4	200, 200	105, 105	2, 6	[22]
22	JPC43	2.0 to ~0 ka BP	2.35	100	51	5	[24]
23	TPC522	2.0 to ~0.8 ka BP	0.33	240	133	4	[25]
24	KROCK-125-GC2	2.0 to ~0 ^{14}C ka BP	0.9	100	51	5	[26]
25	GC1	2.0 to ~0 ka BP	0.5	200, 200	105, 105	2, 5	[27]
26	JPC41	2.0 to ~0 ka BP^	12	<1^		2	[28]
27	GC 5	1.3 to ~0 ^{14}C ka BP	0.14	700	175	2	[29]
28	KROCK-128-GC1	2.0 to ~0.2 ^{14}C ka BP	0.65	100	51	5	[26]
29	CB2010	0.25 to ~0 ka BP	1.4	6, 6	3, 3	7, 8	[30]
30	PG1433	2.0 to ~0.3 ka BP	2.18	85	44	6	[31]
31	PG1430	2.0 to ~0 ka BP	2.65	100	51	6	[31]
32	MD03-2597	2.0 to ~0.7 ka BP^	20.54	<1^		5	[32]
33	DTCI2010; 318-1357B	0.04 to ~0 ka BP; 2,0 to 0.1 ka BP **	18.13, 19.14	19, 0.4, 19, 0.4	10, <0.4, 3, <0.4	1, 7, 8, 8	[33,34]
34	PG1173	2.0 to ~0 ka BP	1.45	50	20	5	[35]
35	MD03-2601	2.0 to ~1.0 ka BP	5	10, 25, 10, 25, 25, 50	<10, 10, <10, 10, 10, 26	1, 4, 5, 5, 7, 8	[20,36–39]
36	WAP13-GC47	2.0 to ~0.1 ka BP	0.84	190	100	4	[40]
37	JPC10/178-1098	2.0 to ~0.2 ka BP, 2.0 to 0 ka BP **	1.16, 2.00	173, 100, 100, 43	91, 51, 51, 17	1, 5, 7, 8	[41–43]
38	PD92-30	2.0 to ~0.3 ^{14}C ka BP	2.82	85, 85	44, 44	1, 3	[44,45]
39	TC46/GC47	2.0 to ~0.1 ka BP	0.42	100	190	4	[46]
40	MTC18A	0.13 to ~0 ka BP	3.46	3, 3	1, 1	5, 8	[47]
41	GC 02	2.0 to ~0.9 ^{14}C ka BP	0.16	220, 220	122, 122	3, 5	[48]
42	KC2B	2.0 to ~0 ka BP	1.15	200	105	6	[49]
43	MTC38C, JPC38	0.08 to ~0 ka BP, 2.0 to ~0 ka BP **	5.75, 2.5	2, 2, 50, 20	<1, <1, 20, <20	5, 8, 5, 8	[47,50]
44	PC61	2.0 to ~0 ka BP	0.5	200	105	2	[51]
45	JPC02	2.0 to ~0 ka BP	11	200	105	7	[52]
46	A-3	1.7 to ~0 ka BP	2.59	85	44	5	[53,54]
47	JPC36	0.8 to ~0 ka BP	17.5	40, 40	21, 21	5, 7	[55]
48	GC 03	2.0 to ~0.1 ^{14}C ka BP	0.32	188, 188	99, 99	3, 5	[48]
49	A-6	1.8 to ~0.1 ka BP	0.81	80	41	5	[53,54]
50	Gebra-1	2.0 to ~0.2 ka BP	0.72	90	46	5	[53,56]
51	1B	2.0 to ~0.1 ka BP	4.21	950	475	7	[57]
52	MC-01	1.7 to ~0 ^{14}C ka BP	2.18	17, 17	<17, <17	2, 7	[58]
53	WB2	1.5 to ~0 ^{14}C ka BP	1.8	38	15	2	[59]
54	CB2	2.0 to ~0 ^{14}C ka BP	2.2	20, 20	<20, <20	2, 7	[60]
55	Gebra-2	1.6 to ~0.1 ka BP	2.93	90	15	5	[53,56]
56	13PC (TN057-13PC4)	2.0 to ~0 ka BP	0.35	20	<20	5	[61]
57	E27-23	2.0 to ~1.5 ka BP	0.5	500	100	5	[62]
58	PS1652-2	2.0 to ~0.6 ka BP	0.64	280, 280	156, 156	1, 5	[63]
59	PS1768-8	2.0 to ~0.8 ka BP	0.1	600, 600	300, 300	1, 5	[63]
60	177-1094/PS2090-1	2.0 to 1.0 ka BP, 2.0 to ~0.8 ka BP **	0.25, 0.30	240, 500, 240	133, 250, 133	1, 1, 5	[63,64]
61	PS2102-2	2.0 to ~0.2 ka BP	0.32	190, 190	100, 100	1, 5	[63]
62	17PC (TN057-17PC1)	2.0 to ~0.0 ka BP	0.25	40	16	5	[61]
63	COR1GC	2.0 to 1.0 ka BP	0.25	52, 52	26, 26	5, 5	[65]
64	HLF17-1	2.0 to 0.0 ka BP	7.25	20, 20	<20, <20	7, 8	[66]
65	PS97/056-1	0.17 to ~0 ka BP	2	17, 17, 9	9, 9, 4	2, 5, 8	[67]
66	PS97/068-2	0.22 to ~0 ka BP	1.95	11, 11, 6	6, 6, 2	2, 5, 8	[67]
67	PS97/072-2	0.19 to ~0 ka BP	2.05	10, 10, 5	6, 6, 2	2, 5, 8	[67]
68	DTG2011	0.42 to ~0 ka BP	11.17	4, 4	<4, <4	1, 8	[68]

SR—sedimentation rate(s); AP—Antarctic Peninsula; 14C ka BP = corrected 14C age, ka BP = calendar age (based on calibrated C14 dates, Pb210 ages and/or extrapolated from sedimentation rates). * Where more than one age model published, the one in calendar years or the most recent is used; ** Different age ranges are listed in order of publication. ^ Discrete sample horizons from laminated sediments—date range is not representative and resolution is discontinuous. Δ Resolution calculated from minimum & maximum number of samples (2 to 5, 6 to 10, 11 to 20, 21 to 40, 41 to 100, >100) divided by the age interval (≤2 ka). † Proxy categories are listed in Table 3.

2.1.2. *Fragilariopsis curta* %

Leventer et al. [11] assigned *F. curta* as the most diagnostic diatom species for sea ice reconstructions in the southern Ross Sea (Sites 1, 3, and 4) with relative abundances of >60%

in areas where sea ice cover persists for 10–11 m/y [12]. In contrast with other regions of the Antarctic continental shelf, *F. cylindrus* is considered more indicative of open water conditions in the Ross Sea, with the transition from open water to dense pack ice reflected in a shift in the dominant diatom species from *F. cylindrus* to *F. curta* [11]. Subsequent studies in the Ross Sea (Sites 2, 5–9, and 12) have continued to use *F. curta* % as the prevalent species to infer seasonal sea ice conditions [12–14]. Beyond the Ross Sea, *F. curta* % has been used as the principal taxa to reconstruct sea ice conditions in Prydz Bay (Site 13) [16], the Ingrid Christensen coast (Sites 18 and 21) [22], the MacRobertson Shelf (Sites 26 and 27) [28,29], and the Antarctic Peninsula (Sites 25, 44, 52–54, and 65–67) [27,51,58–60]. Maximum sample intervals of the *F. curta* % records range between 17 and 400 years. In the northern Antarctic Peninsula and Ross Sea, there are six records with sample resolution of 50 years or less (Sites 8, 9, 12, and 52–54). Except for the study of discrete laminations [32], sites on the MacRobertson Shelf and in Prydz Bay have records with maximum sample intervals of 200 to 400 years. The highest resolution record of *F. curta* % (sampling intervals of $\leq$17 years) is from Marian Cove in the South Shetland Islands (Site 52) and covers the past 1.7 ka BP [58]. The other *F. curta* % records cover 0.5 to 2.0 ka of the past 2.0 ka BP with basal ages ranging from 2.0 ka BP to 0.5 ka (Figure 3 and Table 4).

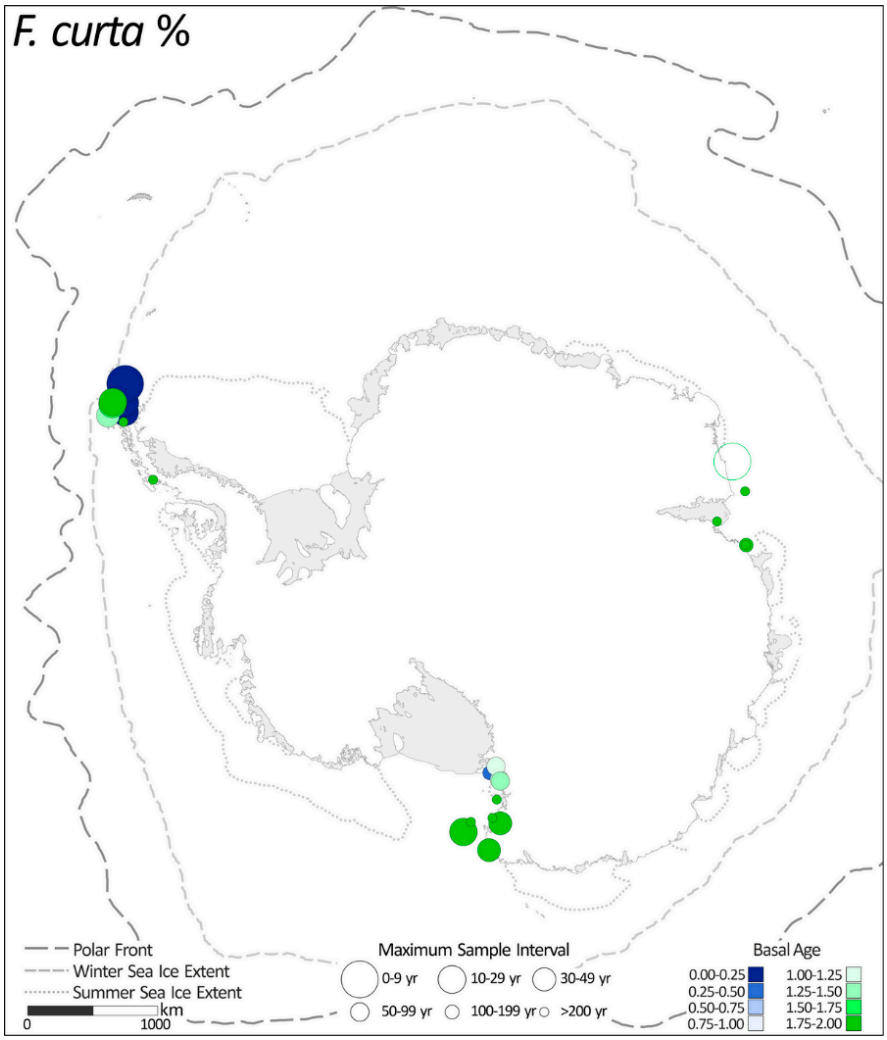

Figure 3. Map showing cores sites where *F. curta* % is used to reconstruct sea ice conditions. The symbol size reflects the resolution of the record and the color of the symbol indicates the basal age of the record between 0 and 2 ka BP. The hollow circle symbols are used for discrete and/or discontinuous records from laminated sediments to illustrate the resolution only.

2.1.3. *Fragilariopsis curta + F. cylindrus/T. antarctica*

The *F. c + cy/T. antarctica* ratio was first applied by Leventer et al. [45] to characterize the overall changes in diatom assemblage and to limit the impact of large relative abundance shifts in other diatom taxa. In the Palmer Deep (Site 38), an increase (decrease) in the ratio suggests greater (lesser) importance of sea ice melt on surface ocean conditions [44,45].

The *F. c + cy/T. antarctica* proxy has only been used at two other sites (Sites 41 and 48), both in the Antarctic Peninsula [48]. Located on the Anvers Shelf, these sites are immediately offshore from the Palmer Deep and comprise records covering 1.1 and 1.9 ka from 2.0 ka BP with sample intervals between 99 and 220 years (Figure 4 and Table 4). The Palmer Deep record (Site 38) covers from 2.0 ka BP to 0.3 ka BP with maximum sample intervals of 85 years [44,45].

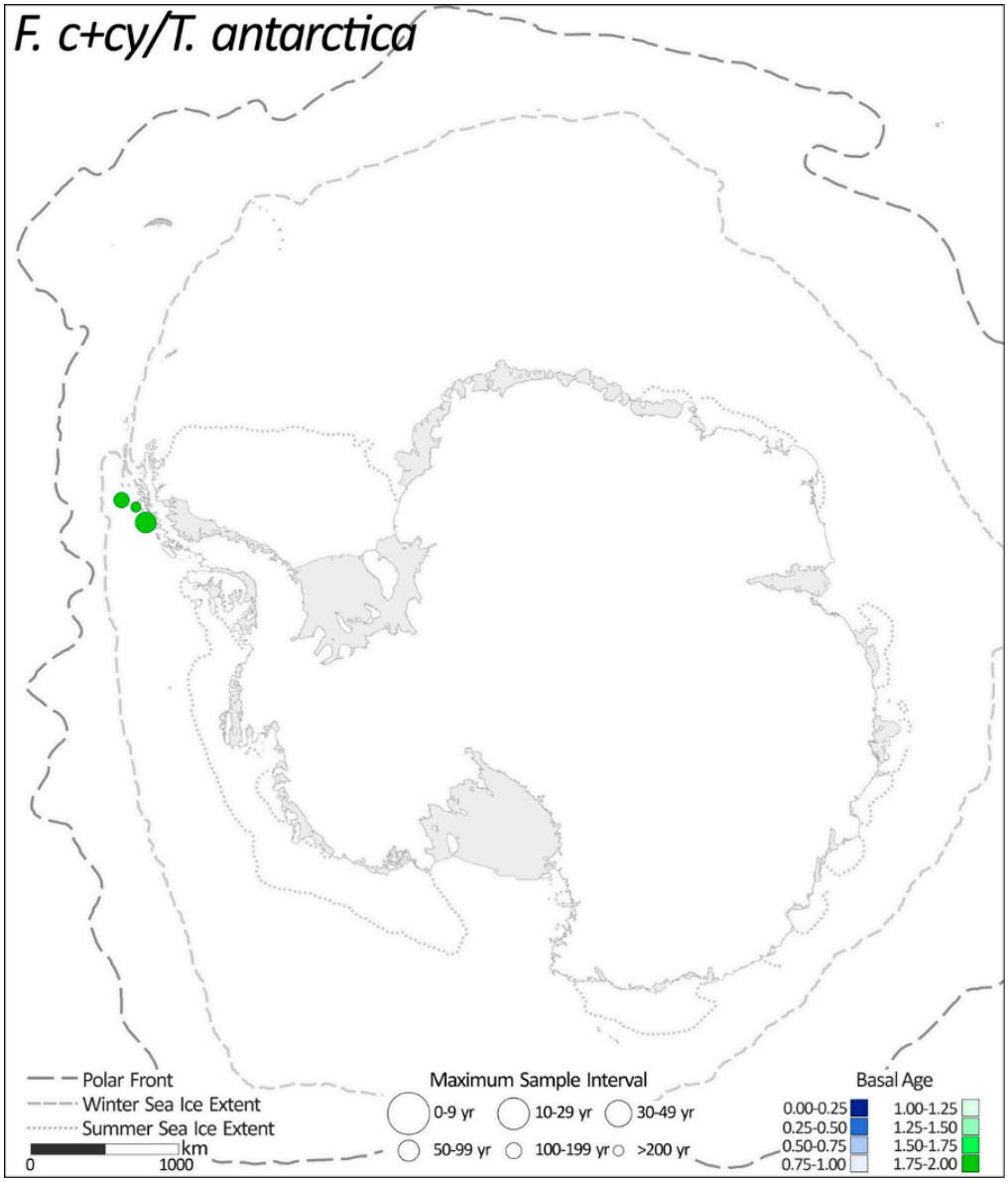

Figure 4. Map showing cores sites where *F. c + cy/T. antarctica* is used to reconstruct sea ice conditions. The symbol size reflects the resolution of the record and the color of the symbol indicates the basal age of the record between 0 and 2 ka BP.

2.1.4. *Fragilariopsis curta/Fragilariopsis kerguelensis*

Similar to the application of the *F. c + cy/T. antarctica* ratio, the *F. curta/F. kerguelensis* ratio was introduced by Denis et al. [39] to reflect the relative dominance of sea ice or sea ice-free conditions in the growing season. Used to interpret the high accumulation sediment record from the Adélie margin (Site 35), *F. curta* and *F. kerguelensis* were chosen based on their elevated abundance in the diatom assemblages and their respective affinities for sea ice and open water conditions.

The *F. curta/F. kerguelensis* ratio has also been applied to infer past sea ice conditions at three other sites (Sites 23, 36, and 63) in the Antarctic Peninsula [25,40,46]. All four *F. curta/F. kerguelensis* records span from 2.0 ka BP (Figure 5 and Table 4), extending to 1.0 ka BP (Site 35) [39], 1.2 ka BP (Site 36) [40], and 1.9 ka BP (Sites 23 and 63) [25,46]. The highest resolution *F. curta/F. kerguelensis* record is presented for the Adélie margin record (Site 35) [39] with sample intervals between 10 and 25 years. The sites from the Antarctic Peninsula (Sites 23, 36, and 63) all have maximum sample intervals between 100 and 230 years (Figure 5 and Table 4).

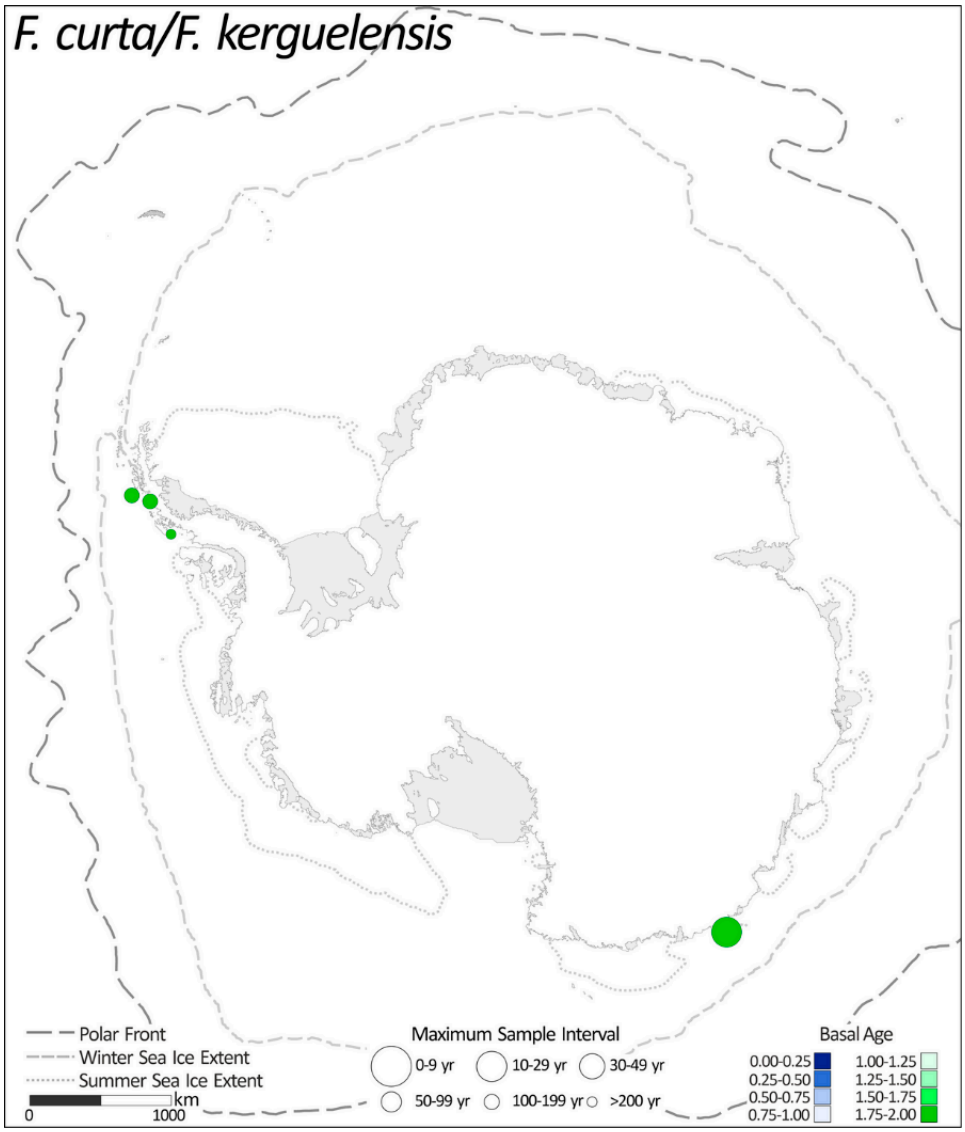

Figure 5. Map showing cores sites where *F. curta/F. kerguelensis* is used to reconstruct sea ice conditions. The symbol size reflects the resolution of the record and the color of the symbol indicates the basal age of the record between 0 and 2 ka BP.

2.1.5. Groups including *Fragilariopsis curta*

A summary of the *F. curta* groups used as sea ice proxies in the records considered here (Table 5) show that there are up to 17 different compositions with at least three species in each. The most common taxa accompanying *F. curta* in the various groups are: *F. cylindrus*, *F. vanheurckii*, *F. obliquecostata*, *F. sublinearis*, *F. rhombica*, *F. ritscheri* and *Porosira glacialis*. Of the other diatom taxa included in the various *F. curta* groups, several are only used at one site within a single study, including *Berkeleya rutilans*, *Cocconeis* spp., *Corethron* spp., *Entomoneis kufferathii*, *Eucampia antarctica* and *Synedra* spp. The remaining taxa (e.g. *Actinocyclus actinochilus*, *Chaetoceros* resting spores (CRS), *Pseudonitzschia turgiduloides*, *Fragilariopsis kerguelensis, Pentalamina corona*, *Thalassionema* spp., *Thalassiosira antarctica, T. lentiginosa, T. tumida* and *Thalassiothrix antarctica* etc.) are included within the 'sea ice groups' of at least two sites within this category.

Table 5. Composition of proxy groups including *Fragilariopsis curta*.

Composition	Sites	References
Fragilariopsis curta, *F. cylindrus*, *Navicula glaceii*, and *F. rhombica*.	14, 15	[17]
Fragilariopsis curta, *F. cylindrus, F. sublinearis*, *F. obliquecostata*, *F. vanheurckii*, and *Porosira glacialis*	16, 35	[18,19]
Cluster groups: Coastal-CRS—*Fragilariopsis curta, F. cylindrus, F. rhombica*, and *Pseudonitzschia turgiduloides*; Shelf-CRS—*F. curta, F. cylindrus, F. rhombica, Pentalamina corona* [a], *Porosira glacialis*, and *Thalassiosira antarctica*	17, 24, 28	[21,26]
PCA: *Fragilariopsis curta, F. cylindrus, F. obliquecostata*, *F. ritscheri, F. sublinearis*, and *F. vanheurckii*	22	[24]
Cluster group 1: dominated by *Thalassiosira antarctica* (T1 and T2) and *Fragilariopsis curta*, with *F. cylindrus, F. rhombica, Navicula* spp., *Pentalamina corona* [a], *Pseudonitzschia turgiduloides, Rhizosolenia* spp., and *Synedra* spp. also present	25	[27]
Spring sea ice represented by laminae types A1, A2, and A3: CRS and *Fragilariopsis* spp. (with *F. curta, F. cylindrus*, and *F. rhombica* dominant)	32	[32]
Actinocyclus actinochilus, Berkeleya rutilans, Entomoneis kufferathii [b], *Eucampia antarctica, Fragilariopsis angulata* [c], *F. curta, F. cylindrus, F. obliquecostata, F. ritscheri, F. sublinearis, Porosira glacialls, P. pseudodenticulata*, and *Distephanus speculum* [d]	34	[35]
The *Fragilariopsis curta* group: *F. curta, F. cylindrus*, and *F. vanheurckii*; and the *Fragilariopsis* cryophilic group: *F. obliquecostata*, *F. ritscheri*, and *F. sublinearis*	35	[38]
Cluster groups: *Cocconeis* assemblage dominated by *Fragilariopsis curta* and *Thalassiosira antarctica*, with *Cocconeis* as a unique indicator, and *Corethron* assemblage dominated by *F. curta* and *F. cylindrus*, with *Corethron* spp. and *Pseudonitzschia turgiduloides* as indicators	37	[43]
Fragilariopsis curta, *F. cylindrus*, and *F. vanheurckii*	40, 43	[47]
Sea ice taxa (not itemised) assume at least: *Fragilariopsis curta* and *F. cylindrus* (based on the use of '*F. c + cy/T. antarctica*' ratio in the same publication)	41, 48	[48]
Fragilariopsis curta, *F. cylindrus, F. sublinearis*, and *F. vanheurckii*	43, 47	[50,55]
The sea ice taxa group: *Fragilariopsis curta*, *F. cylindrus, F. sublinearis, F. obliquecostata*, and *F. vanheurckii*	46, 49, 50, 55	[53,54,56]
MAT (31–33 taxa): *Actinocyclus actinochilus, Alveus marinus* [e], *Azpeitia tabularis*, the *Chaetoceros resting spore* group, *Fragilariopsis curta, F. cylindrus, F. doliolus, F. kerguelensis, F. obliquecostata, F. rhombica, F. ritscheri, F. separanda, F. sublinearis, Hemidiscus cuneiformis, Porosira glacialis, P. pseudodenticulata, Rhizosolenia antennata* f. *semispina, R. styliformis, Roperia tesselata, Stellarima microtrias, Thalassionema nitzschioides, T. nitzschioides* var. *lanceolata, T. nitzschioides* var. *parva*, the *Thalassiosira antarctica* group (warm and cold morphologies [e]), the *T. eccentrica* group, *Shionodiscus gracilis* [f], *T. lentiginosa, S. oestrupii* [f], *T. oliveriana, T. tumida, Thalassiothrix* spp., and *Trichotoxon reinboldii* [72,73]	56, 62, 63	[61,65]
GAM: *Actinocyclus actinochilus, Fragilariopsis curta, F. cylindrus*, and *Thalassiosira lentiginosa*	57	[62]
MAT (28 taxa): *Actinocyclus actinochilus, Azpeitia tabularis, Fragilariopsis curta, F. cylindrus, F. doliolus, F. kerguelensis, F. obliquecostata, F. rhombica, F. ritscheri, F. separanda, F. sublinearis, Hemidiscus cuneiformis, Nitzschia bicapitata, Porosira pseudodenticulata, Pseudonitzschia turgiduloides, Rhizosolenia* spp., *R. antennata* f. *semispina, R. bergonii, Roperia tesselata, Thalassionema nitzschioides* f. *1, T. nitzschioides* var. *parva, T. nitzschioides* var. *lanceolata* + *T. nitzschioides* var. *capitulata, Thalassiosira antarctica, Shionodiscus gracilis* [e], *T. lentiginosa, S. oestrupii* [e], *T. oliveriana*, and *Thalassiothrix antarctica* [70]	58, 59, 60, 61, 65, 66, 67	[63,67]
The sea ice group: *Fragilariopsis curta, F. cylindrus, F. obliquecostata, F. ritscheri, Porosira glacialis*, and *Thalassiosira tumida*	63	[65]

a—Bolidophyceae Parmales; b—Synonym: *Amphiprora kufferathii*: c—Synonym: *F. rhombica*; d—Silicoflagellate; e—excluded from MAT-31 f—previously assigned to *Thalassiosira* genus.

The *F. curta* groups have been applied as proxies for sea ice throughout the Antarctic, including the deep Southern Ocean (Sites 56–62), the Antarctic Peninsula (Sites 22, 25, 37,

40, 41, 43, 46, 47, 48, 49, 50, 52, and 55), and the EA margin (Sites 14, 15, 16, 17, 24, 28, 32, 34, and 35).

The majority (n = 27) of the 36 records using a *F. curta* group as a sea ice proxy date back to at least 2 ka BP, of which 11 cover the entire 2 ka period. The 9 records that start after 2 ka BP include 3 that span more than 1.5 ka and 6 records that cover between 0.8 and 0.08 ka BP to the present (Figure 6 and Table 4). One *F. curta* group record (Site 32) from the Dumont D'Urville Trough characterizes the seasonal sequence of sea ice and open water production from specific intervals of Late Holocene laminated sediments [32], whilst all other *F. curta* group records have maximum and minimum sample intervals ranging from 1000 to 2 years and 500 to 1 year, respectively (Figure 6 and Table 4).

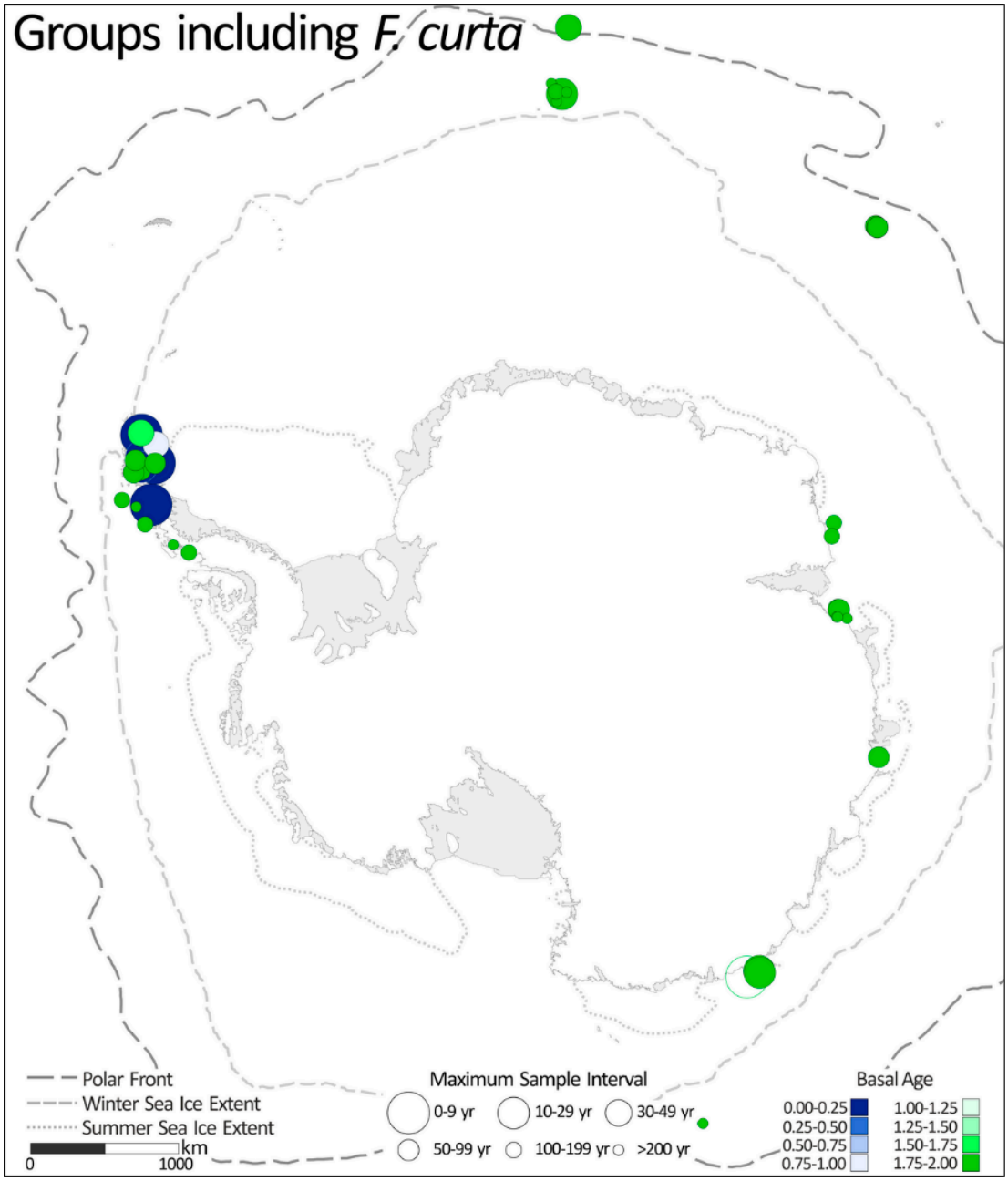

Figure 6. Map showing cores sites where groups of taxa including *F. curta* are used to reconstruct sea ice conditions. The symbol size reflects the resolution of the record and the color of the symbol indicates the basal age of the record between 0 and 2 ka BP. The hollow circle symbols are used for discrete and/or discontinuous records from laminated sediments to illustrate the resolution only.

2.1.6. Groups Excluding *Fragilariopsis curta*

There are seven proxy records based on three groups of diatoms excluding *F. curta* (Table 6). Each of the groups excluding *F. curta* are comprised of a unique set of taxa (Table 5), with only *N. glaceii* incorporated in groups both including and excluding *F. curta* (Tables 5 and 6). The habitat preferences of these species are available in Appendix A.

Table 6. Composition of proxy groups excluding *Fragilariopsis curta*.

Composition	Sites	References
Fast ice index: *Entomoneis kjellmannii, Nitzschia stellata, Berkeleya adelienses, Thalassiosira australis, Pleurosigma directum* and *Pinnularia quadreata*	18–21	[22,23]
Fragilaria striulata, Navicula glaceii, and *Synedropsis* spp.	30, 31	[31]
Prolonged sea ice inferred from *Navicula* spp.	42	[49]

The seven records utilizing the three 'non-*F. curta* groups' to infer sea ice conditions are presented for coastal sites of the Vestfold Hills (Sites 18–21), Wilkes Land (Sites 30 and 31), and James Ross Island (Site 42) In many of these coastal settings, *F. curta* is considered more indicative of 'open water' conditions rather than extensive pack or fast ice [17,22]. All records date back to at least 2 ka BP, with three records that span the complete 2.0 ka interval (Sites 42, 31, and 18), two that are continuous through to 0.8 ka BP (Sites 20 and 21), one that covers up to 0.3 ka BP (Site 30), and one that covers up to 0.2 ka BP (Site 19). Across the seven sites, maximum sample intervals range between 200 and 30 years and minimum sample intervals range from 105 to 12 years (Figure 7 and Table 4).

2.1.7. Other

Records in this category are based on generic features of the diatom assemblage; distinct qualities of a single taxa; or reconfigured versions of the proxies described in proxy categories 1–4 (Table 7). The habitat preferences of these species are presented in Appendix A.

- *Entomoneis kjellmannii* % (previously *Amphiprora kjellmannii*) is primarily used as an indicator of perennial sea ice, especially fast ice [17,22,23]. *E. kjellmannii is* reported as a common, sometimes dominant, member of the sea ice diatom community in coastal areas of the Ross Sea and is also abundant in the sea ice and sea ice adjacent waters of the Ingrid Christensen coast and in parts of the Victoria Land coast [74–76]. *E. kjellmannii* is a component of the 'fast ice index' (one of the non-*F. curta* groups—Section 2.1.6 and Table 6) presented by McMinn [22] and McMinn et al. [23] and used by Berg et al. [17] as evidence for the presence of fast ice on the Rauer Group coast, Prydz Bay.
- *Eucampia* index is introduced by Kaczmarska et al. [77] and based on the distinct morphology of the 'pointed' or 'horned' terminal valves and 'flat' intercalary valves of both the polar *E. antarctica* var. *recta* and the sub-polar *E. antarctic* var. *antarctica* morphotypes [78]. The *Eucampia* index refers to the ratio of terminal to intercalary ('pointy to flat') valves. *E. antarctica* colonies growing in colder waters with greater sea ice cover are characterized by shorter chains with a higher relative proportion of terminal valves [79,80]. Milliken et al. [57] use the *Eucampia* index to infer changes in sea ice cover over Maxwell Bay in the South Shetland Islands (Site 51). Resolution of this record ranges between 475 and 950 years and spans between 2.0 and 0.1 ka BP (Figure 8 and Table 4).
- *Fragilariopsis cylindrus* % is used as the primary indicator of prolonged sea ice cover (>8.5 months) by Campagne et al. [30,33], owing to *F. cylindrus*'s high statistical significance in explaining variability in the diatom assemblages of the past 40 years in the Adélie Margin (Sites 29 and 33) where *F. curta* was not significant. Yoon et al. [58,60] present separate down-core abundance plots for *F. curta* and *F. cylindrus*% (Sites 52

and 54), showing that peaks are often off-set and highlighting the sensitive habitat preferences of the two species.

- The *Fragilariopsis* group/*Thalassiosira antarctica* (T2) is similar to the more commonly applied *F. curta* + *F. cylindrus*/*T. antarctica* ratio. The *Fragilariopsis* group/*T. antarctica* (T2) ratio also aims to characterize the major shifts in surface ocean conditions with elevated (reduced) contributions of the *Fragilariopsis* group (*T. antarctica*) indicative of more persistent (ephemeral) seasonal sea ice. As presented in Kamanidou et al. [55], the *Fragilariopsis* group comprises of the combined abundance of *F. curta*, *F. cylindrus*, *F. sublinearis*, and *F. vanheurckii*. Applied to the sediment record from the Perseverance Drift north of Joinville Island in the northern-most Antarctic Peninsula (Site 47), the record covers from 0.8 to 0.0 ka BP at a resolution between 40 and 21 years [55].
- *Porosira glacialis*/*Thalassiosira antarctica* are both common components of the diatom assemblage in Antarctic continental shelf sediments with *P. glacialis* preferring slightly cooler ocean climate conditions than *T. antarctica* [81,82]. As established by Pike et al. [20], the ratio of *P. glacialis*/*T. antarctica* reflects the subtle difference in environmental preferences of the two species, with ratios of >0.1 indicating annual sea ice cover greater than 7.5 months/year [20]. Applied to sediment records from the Svenner Channel, Prydz Bay, and the Dumont d'Urville Trough (Sites 16 and 35), the *P. glacialis*/*T. antarctica* ratio is used to reconstruct changes in the duration of sea ice cover [20]. The record from the Svenner Channel (Site 16) covers between 2.0 and 0.6 ka BP with a maximum and minimum resolution of 36 and 70 years, respectively [20]. The Dumont d'Urville record (Site 35) spans the period from 2.0 to 1.0 ka BP with sample intervals between 25 and 2 years [20].
- Pennate–centric ratio—in sediments with low diatom concentrations, Minzoni et al. [15] use the prevalence of pennate diatoms in the assemblage to infer the presence of sea ice. The association between elevated contributions of pennate diatoms and heavier sea ice cover is based on analyses of the core top assemblages that are dominated by *F. curta* [83]. Applied to cores recovered from Ferrero Bay in the Amundsen Sea Embayment (Sites 10 and 11) where sedimentation rates are exceptionally low for the AP, the records of the pennate–centric ratio cover the whole of the last 2 ka at both sites with sample intervals of 500 to 1000 years (Figure 8 and Table 4).
- Diatom concentrations—Sjunneskog and Taylor [42] and Michalchuk et al. [52] use diatom concentrations as a paleoproductivity proxy for the Palmer Deep and Firth of Tay marine cores (Sites 37 and 45) based on the dominant contribution of the sea ice melt bloom to the total diatom production which is reflected in the prevalence of *Chaetoceros* resting spores (60 to 90% of the total diatom content) in AP sediments [45,84].
- Dark–light laminae—in laminated sediments from Edisto Inlet in the Ross Sea (Site 64) Tesi et al., [66] show that dark and light layers are characterized by distinctive diatom assemblages, biomarkers, and isotopic values that reflect the two dominant seasonal sea ice settings of the site: (1) sea ice break-up and thaw (dark) and (2) open surface waters (light). Tesi, et al.'s [66] record spans the last 2 ka with sample intervals of <20 years (Figure 8 and Table 4).

Table 7. Composition of all 'other' diatom proxies.

Composition	Sites	References
Entomoneis kjellmanii %	14 and 15	[17]
Eucampia index	51	[57]
F. cylindrus %	29, 33, 52, and 54	[30,33,58,60]
F. group/*T. antarctica (T2)*	47	[55]
Porosira glacialis/*T antarctica*	16 and 35	[20]
Pennate–centric ratios	10 and 11	[15]
Diatom concentrations	37 and 45	[42,52]
Frequency of dark–light laminae	64	[66]

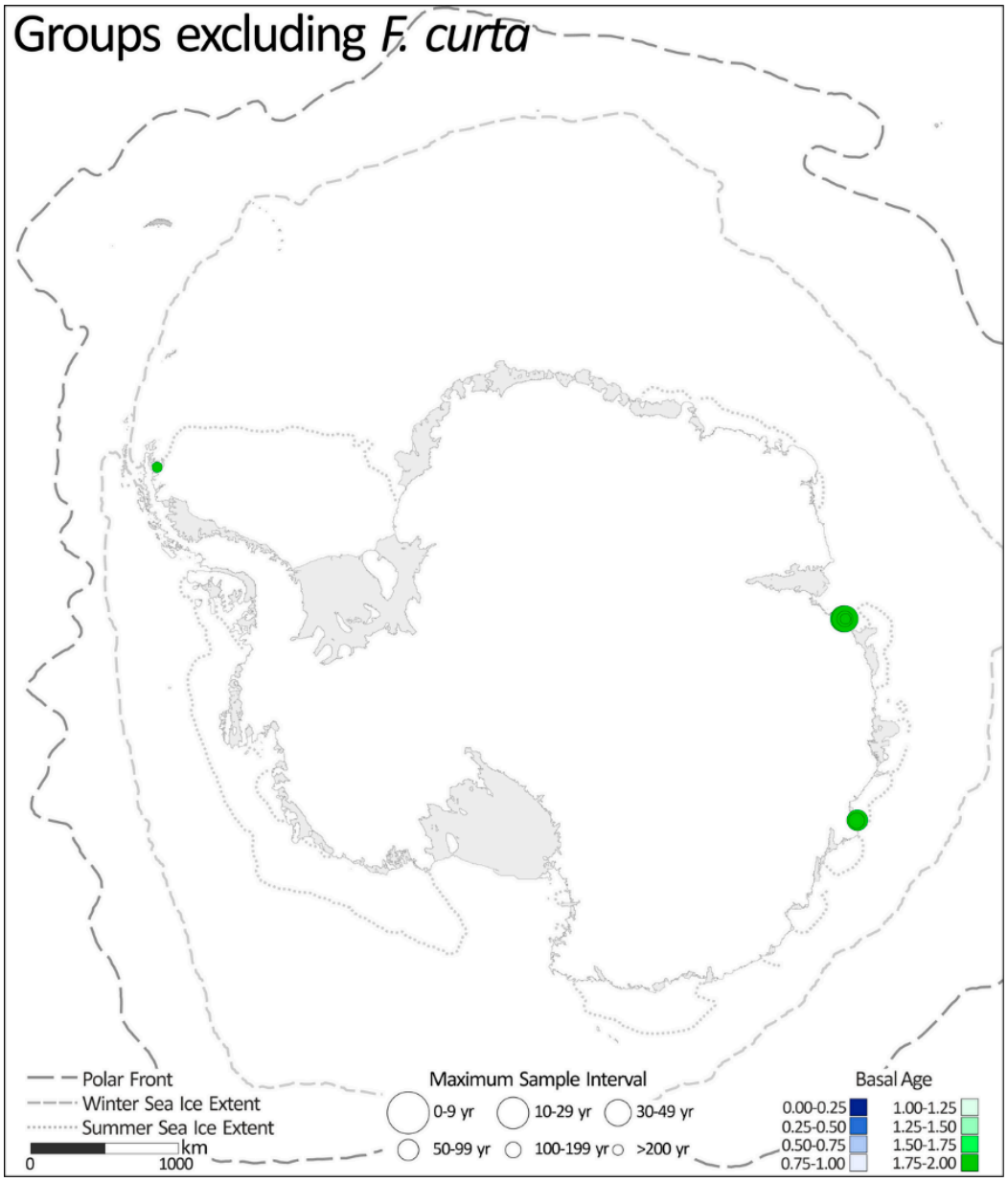

Figure 7. Map showing cores sites where groups of taxa excluding *F. curta* are used to reconstruct sea ice conditions. The symbol size reflects the resolution of the record and the color of the symbol indicates the basal age of the record between 0 and 2 ka BP.

2.1.8. Diatom-Specific Highly Branched Isoprenoids (HBIs)

The use of HBIs as a source-specific biomarker for sea ice was first developed in the Arctic where IP25 (a mono-unsaturated C_{25} HBI, HBI-I) is produced by three or four sea ice diatoms [85,86]. Whilst IP25 has not been identified in Antarctic sediments, a di-unsaturated C_{25} HBI (diene, HBI-II) found to co-vary with IP25 in the Arctic [87–90] has been identified in sediments and sea ice from a variety of Antarctic locations [19,91–97]. In 2016, Belt et al. [10] established that the sympagic diatom *Berkeleya adeliensis* is a principal source of this diene (HBI-II) and proposed the term IPSO25 (ice proxy for the Southern Ocean with 25 carbon bonds) by analogy to the Arctic IP25. Analysis of its distribution in near-coastal Antarctic sediments led to the conclusion that IPSO25 may be a better proxy of the type of sea ice in which it is produced (platelet ice) rather than other parameters such as sea ice extent or seasonality [10,98].

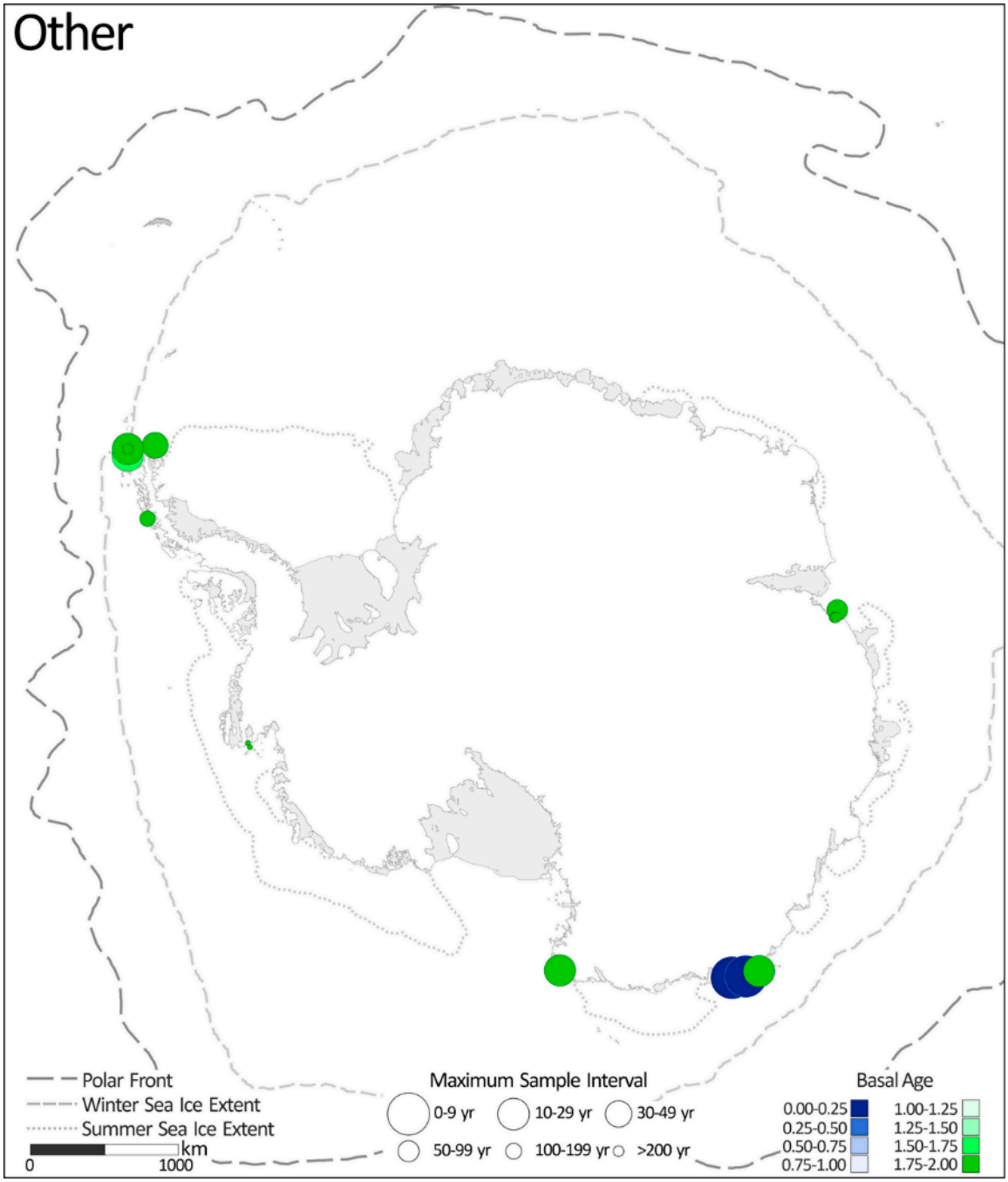

Figure 8. Map showing cores sites where all other proxies based on diatom taxa are used to reconstruct sea ice conditions. The symbol size reflects the resolution of the record and the color of the symbol indicates the basal age of the record between 0 and 2 ka BP.

A third tri-unsaturated C25 HBI (triene, HBI-III) was initially proposed to derive from open water taxa [94]. As such, the ratio between the diene and triene (HBI-II/HBI-III) was thought to reflect the relative contributions of sea ice and open ocean primary production [19,91,94]. Subsequent studies have suggested that the production of triene (HBI-III) may instead be concentrated in the marginal ice zone [50,93]. For more information on the use of HBI-II and HBI-III as sea ice proxies, readers are encouraged to consult the recent review paper by Belt [98].

Within this review, there are 14 HBI records for 12 sites across the Antarctic Peninsula, Prdyz Bay, the Adélie Land shelf, the coast of George V Land, and the western Ross Sea

(Sites 16, 29, 33, 35, 37, 40, 43, 64, 65, 66, 67, and 68) (Figure 9 and Table 4). Of these 14 HBI records, 4 span from 2.0 ka BP to 1.0, 0.6, 0.3 and0.1 ka BP, 2 span to 0.0 ka BP, whilst the other 8 records begin at 0.42, 0.25, 0.22, 0.19, 0.17, 0.13, 0.08, and 0.03 ka BP, only covering the most recent centuries and decades. The lowest sample resolution for the 6 records covering older sediments range between 70 and <20 years, whilst the largest sample interval for the younger core archives ranges between 9 and 0.4 years.

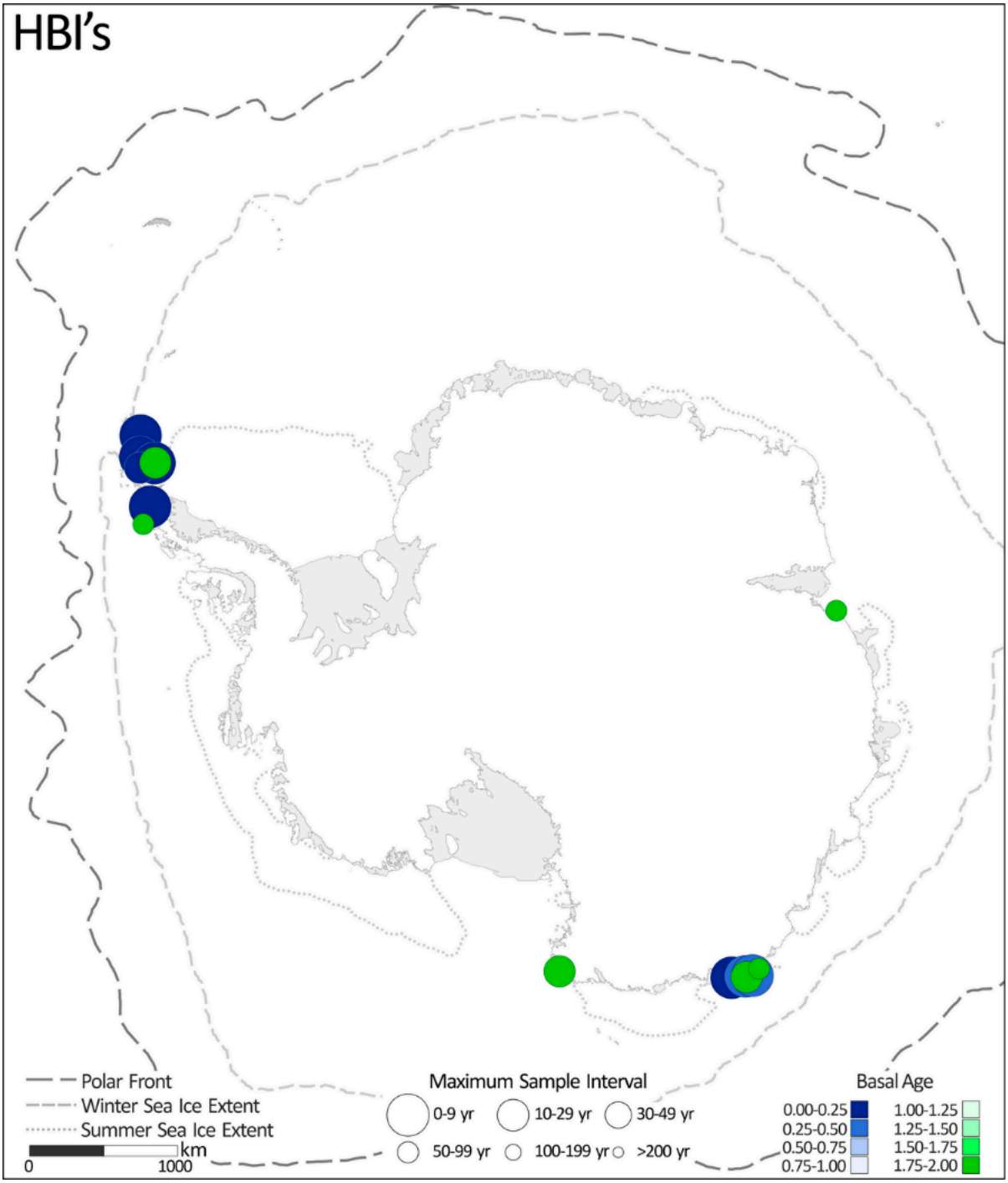

Figure 9. Map showing cores sites where highly branched isoprenoids (HBIs) are used to reconstruct sea ice conditions. The symbol size reflects the resolution of the record and the color of the symbol indicates the basal age of the record between 0 and 2 ka BP.

2.2. Distribution of Diatom-Based Proxy Records

Whilst diatomaceous sediments are widely available in the deep Southern Ocean and the Antarctic continental shelf, there are large disparities in the distribution of records (Figures 1 and 10). The highest concentrations of sites occur in the northern Antarctica Peninsula and the western Ross Sea. Meanwhile, there are currently no records on the continental shelf between the Larsen Shelf on the eastern Antarctic Peninsula and Enderby Land on the East Antarctic Margin (approx. 60° W to 60° E); there are only two records from the West Antarctic Margin between the Ross Ice Shelf and Alexander Island (approx. 170° E to 70° W); and there are only three coastal records from the Wilkes Land Margin (approx. 80° E to 135° E). This uneven distribution is typical of most Antarctic marine proxy records and largely reflects the availability (and collection) of marine sediment cores from the Antarctic continental shelf and Southern Ocean.

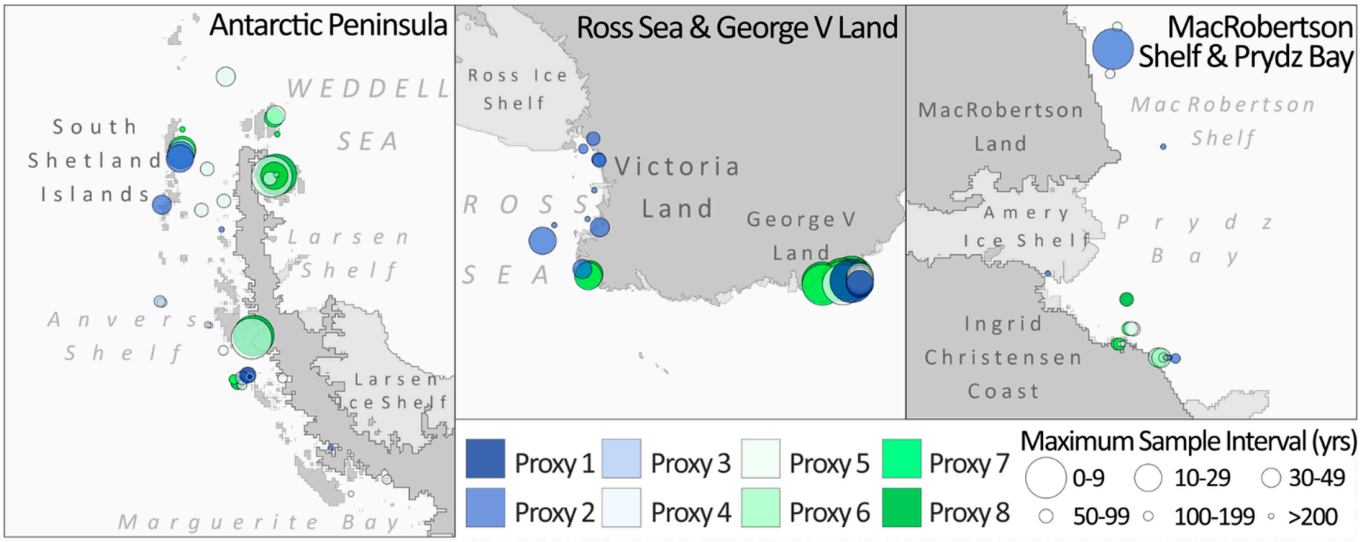

Figure 10. Maps of regions with greatest density of sea ice records from marine sediment cores, showing the diversity of proxy types and sample resolution. The symbol size reflects the resolution of the record and the color of the symbol indicates the proxy type (see Tables 1 and 3).

3. Advantages and Limitations

Diatom-based sea ice proxies from marine sediments provide the most direct link to the Antarctic sea ice environment. The fossilized frustules and biomarkers of diatoms living in or attached to sea ice offer the best evidence of sea ice in marine sediments. Whilst few of these ice-bound diatoms are preserved and most of them are specific to highly niche conditions or particular types of sea ice, there are several diatom species associated with sea ice and water in close proximity with sea ice, which are commonly preserved in Antarctic marine sediments. These taxa hold the greatest potential for a standard/generic sea ice proxy. The main pro's and con's of each proxy category are summarised in Table 8.

3.1. Relative Abundance

Except for HBIs, the relative abundance of species and species groups within the diatom assemblage provides baseline data in 77 of the proxy records used to reconstruct Antarctic sea ice over the past 2 ka.

The interpretation of sea ice proxies based on relative abundance is complicated by the differences in composition of the overall assemblage. Whilst the contribution of sea ice taxa to the total diatom assemblage in sediments from the deep Southern Ocean exhibits a strong latitudinal gradient correlated with sea ice cover [71], the relative abundance of sea ice taxa in Antarctic continental shelf sediment is more diverse. Where sea ice taxa comprise minor taxa (<10%), changes in the relative abundance of dominant/abundant

taxa can erase, reverse, or enhance the relative abundance trends of the proxy [99]. In the Antarctic Peninsula, where *Chaetoceros* spp. frequently comprise >70% of the diatom assemblage [24,27,40,41,43,45,47], it is common practice to mitigate the dominance of *Chaetoceros* spp. by carrying out additional valve counts excluding *Chaetoceros* spp. in order to resolve the abundance patterns of minor taxa. The assemblage variability throughout the continental shelf makes it untenable to assign relative abundance thresholds to specific sea ice conditions (duration, concentration, etc.) and limits inter-site comparison to assess similarities in the timing and pattern of sea ice trends.

Table 8. Summary of main advantages and limitations of the eight proxy types.

Proxy Type	Advantages	Limitations
1. *F. curta* + *F. cylindrus*	Well-established links between *F. curta* and *F. cylindrus* with sea ice melt waters, relative abundance in sediments over large areas of the deep Southern Ocean consistently linked with seasonal sea ice, based on large reference dataset of sediment traps and core tops throughout the deep South Atlantic	Proxy only 'calibrated' for Atlantic sector of the deep Southern Ocean
	Both *F. curta* and *F. cylindrus* are widely preserved in marine sediments of the deep and continental shelf areas of the Southern Ocean	*F. cylindrus* not exclusive to sea ice meltwater but also found in glacial meltwaters and in stratified waters of the Ross Sea
	Can be successfully applied at several sites in the deep South Atlantic and over a variety of late Quaternary timescales	*F. nana* often not differentiated from *F. cylindrus*
	Well-defined morphology that minimizes risks of misidentification	Excludes broader assemblage information
		Small changes in the relative abundances of dominant species can have a pronounced impact on the percentages of minor taxa
2. *F. curta*	Well-established association with seasonal sea ice throughout the deep Southern Ocean and the continental shelf	Association with seasonal sea ice fails over short/annual timeframe
	Widely preserved and common in sediments throughout the deep Southern Ocean and the continental shelf	Relative abundances vary greatly from site to site
	Well-defined morphology that minimizes risks of misidentification	Excludes broader assemblage information
3. *F. c* + *cy*/*T. antarctica*	Ratio reduces influence of % changes in dominant species	Several morphotypes of *T. antarctica* and ambiguity over exact ecological associations—complicate identification and interpretation of ratio
	Well-established association between *F. c* + *cy* and seasonal sea ice (see above)	Subjective boundaries between *T. antarctica* morphotypes compound identification difficulties and in particular compromise cross-site comparison
4. *F. curta*/*F.kerguelensis*	Ratio reduces influence of % changes in dominant species	Abundance of *F. kerguelensis* (strongly silicified) can be increased in sediments affected by dissolution
	F. kerguelensis is well established as an open ocean diatom, so the ratio is a robust indicator for the relative influence of open ocean versus sea ice conditions	

Table 8. *Cont.*

Proxy Type	Advantages	Limitations
5. Groups including *F. curta*	Groups incorporate information of broader assemblage	Difficult to have a group that is appropriate for a wide range of continental shelf sites
	Groups can be tailored to local ocean conditions and/or assemblage composition	Transfer functions primarily built on reference data from deep ocean sites where seasonal sea ice expands and retreats along the north–south axis are not necessarily appropriate for continental shelf sites where sea ice distribution is more complex
	Many groups are statistically defined	Transfer functions only reliable within area of reference sites
	Transfer functions incorporate most species and produce quantitative results	
6. Groups excluding *F. curta*	Groups mostly tailored to specific nearshore conditions or particular types of sea ice	Most groups not suitable for application in offshore regions of the continental shelf or deep ocean regions
	Sensitive to different types of sea ice	Sensitive to different types of sea ice rather than duration or distribution of sea ice cover
7. Other	Many based on routine information that can be applied alongside other species or assemblage proxies (e.g., Diatom concentration, pennate–centric, *P. glaciailis*/*T. antarctica*)	Most are only indirectly linked to sea ice
	Can be widely applied throughout the continental shelf and deep ocean sites	May require additional analyses beyond the standard assemblage composition (e.g., morphometrics of the marine diatom *Eucampia antarctica*)
8. HBIs	Less time-intensive analyses, creating generally higher resolution records than traditional diatom assemblage data	Still requires considerable effort and personnel time to produce records
	Diene (HBI-II) linked to the sea ice diatom *Berkeleya adeliensis*	Absence of diene (HBI-II) can result from both open ocean and permanent sea ice conditions
	Widely preserved in sediments and robust at timescales up to at least 100 ka	Environmental controls on the production of triene (HBI-III) are still ambiguous
		Generally requires some validation with diatom assemblage data to aid interpretation

Ratios between the relative abundance of two diatom species or groups of species provide a way of normalizing data to mitigate the relative abundance differences between sites. A ratio between sea ice taxa and open ocean taxa reflects the prevalence of sea ice over ice-free conditions [45].

3.2. Statistical Approaches

At present, transfer functions (IKM, MAT, and GAM) provide the only quantitative approach to diatom-based sea ice reconstructions. Based on a reference data set of surface sediment samples from sites of varying sea ice conditions, transfer functions provide statistical estimates of past sea ice duration or concentration. The main advantage of transfer functions is that they yield quantitative results that are most easily applied in the set up and validation of climate models. The main limitations for the transfer functions are that the sea ice conditions and diatom assemblages of the continental shelf are typically too varied to be used in transfer functions. Moreover, in the case of IKM and MAT, the assumptions and types of assemblage data applied may not be suitable [100,101].

Other statistical methods applied in diatom-based sea ice reconstructions of the last 2 ka include principal component analyses (PCAs) and cluster analyses. These approaches are used to identify the individual and groups of taxa that are most strongly associated with sea ice and to determine similarities between samples based on their assemblage composition. Results gained from studies applying PCA and cluster analyses benefit from eliminating some of the subjectivity from the process of reconstructing sea ice and use

statistical criteria that can be replicated at sites with different diatom assemblage data. The drawbacks with PCA and cluster analyses are that reconstructions are only qualitative and may reflect the multifaceted environmental gradients linked with sea ice that may complicate the proxy signal.

4. Discussion

4.1. Distribution

The current distribution of marine core sites with sea ice reconstructions for the past 2 ka shows that records are mostly located in the northern AP, the western Ross Sea, and the Prydz Bay area, highlighting the large expanse of the Antarctic continental shelf with no sea ice records of the past 2 ka (Figure 1). The concentration of records in these regions reflects a common bias towards the location of research bases and/or regular supply routes. Regions with fewer Antarctic bases and away from the primary logistic routes have few (Amundsen Sea, the Adelie coast, and the Wilkes Land Coast) or no sea ice records from marine core sites (Dronning Maud Land, Marie Byrd Land, and the southern Bellingshausen and Weddell Seas). Mapping the distribution, basal age, and resolution of proxy records also highlights areas where regional syntheses of centennial-scale sea ice history may be possible and reveals spatial trends in the choice of sea ice proxy that may provide a basis for standardization.

No single proxy is used at all sites. All eight proxy types are applied to sediment cores in the AP and *F. curta* % is used at all sites in the western Ross Sea (Figure 10). 'Groups including *F. curta*' is the most commonly applied proxy type and also the most widely distributed, with records throughout the AP, East Antarctic margin, and deep Southern Ocean (Figure 6). Although each of the 17 distinct groups within this category are only applied at a maximum of four sites (Table 5), the overall distribution attests to where '*F. curta*' is considered useful in reconstructing sea ice. The area where *F. curta* is applied in sea ice reconstructions can be extended by including all proxy records that utilize *F. curta*. This combined distribution illustrates that *F. curta* is used at 57 of the 68 (in 77 of the 112 records) sites across Antarctica (Figure 11). Of the 11 sites where *F. curta* is omitted, 6 are from nearshore fjord and bay settings along the East Antarctic margin (Sites 19, 20, 29, 30, 31, and 64) where the sea ice proxies are tailored to fast ice [23,31,49], 2 are from the Amundsen Sea coast (10 and 11) where diatom concentrations are too low to produce reliable assemblage data [15] and the remaining 4 sites (42, 45, 51, 64) are from studies that promote other features of the sediment cores and/or focus on non-diatom proxies [49,52,57,66].

The paucity of the continental shelf records based on the more established *F. curta* + *cylindrus*% proxy is likely due to two principal factors that complicate the relative abundance patterns of this pairing. Firstly, the diversity of habitats on the continental shelf supports greater variation in the composition, species richness, and evenness of diatom assemblages such that relative abundances are also highly variable. Secondly, the production and distribution of *F. cylindrus* is influenced not only by sea ice but also by cold stratified waters [102–104]. Close to the continent, glacial discharge could produce cold stratified waters and exceed the sea ice influence on the occurrence of *F. cylindrus*, making it unreliable as a sea ice proxy in this setting.

Whilst HBI records have only been applied in recent years, the scope for more efficient analyses of samples and the potential to be included in standard geochemical processing may rapidly increase the application and distribution of this proxy over the next decade. HBIs may also be absent from the sedimentary record and the interpretation of such an absence is often complex. Possible causes include perennial sea ice cover, ice-free conditions, or ice conditions not suitable for diatoms (e.g., the sea ice may be too thick to allow a sufficient amount of light to pass through) [98]. Furthermore, after HBIs have been produced, they must avoid degradation before and after deposition. For example, the incorporation of sulfur into $IPSO_{25}$ may impact some records [95,98] The challenges associated with interpreting such changes have restricted our ability to produce new HBI proxy records.

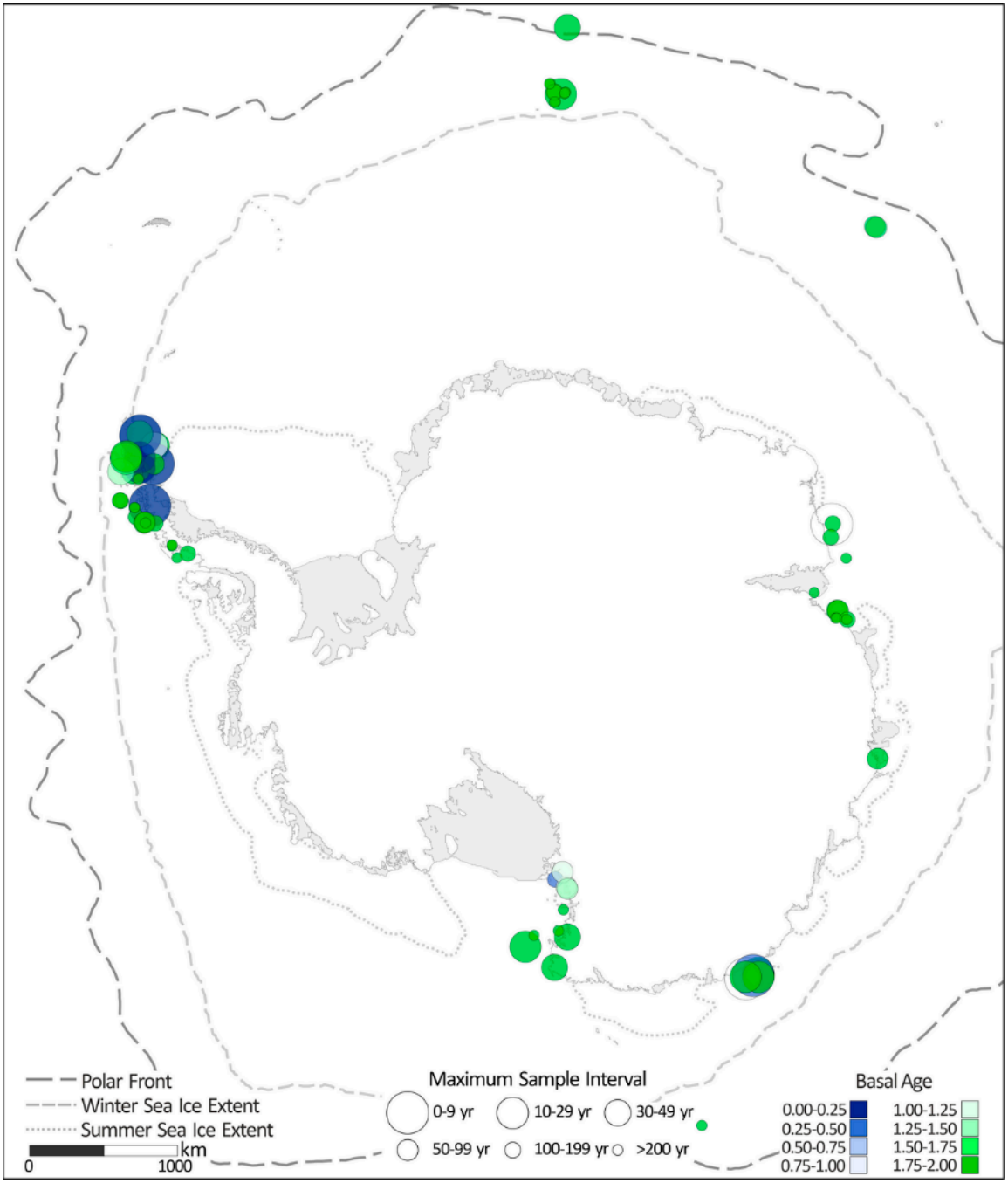

Figure 11. Map of sites that include *F. curta* in at least one proxy record. The symbol size reflects the resolution of the record and the color of the symbol indicates the basal age of the record between 0 and 2 ka BP. The hollow circle symbols are used for discrete and/or discontinuous records from laminated sediments to illustrate the resolution only.

4.2. Age, Duration and Resolution of Records

Many of the Southern Ocean and Antarctic continental shelf records considered here extend beyond the 2 ka interval, with several covering the full Holocene or longer time intervals [13,14,24–26,36,39,41,57,63,105]. Since these sediment cores mostly target millennial to sub-millennial resolutions over a longer timeframe, some may be suitable for higher frequency sampling and dating to improve the resolution and age control of the youngest sediments.

Marine sedimentation rates at many of the sites presented here are considered too low to resolve sub-decadal records. There are rare sites of very high accumulation (~1 cm a^{-1}) on the Antarctic continental shelf that can yield records of sub-decadal to annual resolution (e.g., Site 37/38: IODP 178-1098 and Site 33: IODP 318-1357). Furthermore, where varves are preserved at the highest accumulation sites (2–10 cm a^{-1}), it is possible to resolve seasonal records, usually only for discrete horizons due to the number of samples required and the time-intensive nature of analyses [32,106].

The limits of resolution do not only depend on sedimentation rates but also on signal attenuation from bioturbation. Several studies have explored how bioturbation affects the amplitude, timing, and duration of climate signals in proxy records [107,108]. Whilst the techniques and specific results vary, the studies are broadly consistent in finding substantial attenuation (30 to 70%) in the amplitude of millennial scale climate signals when sedimentation rates are less than ~15 cm ka^{-1}. Similar experiments with centennial and sub-centennial climate variations suggest that a signal is only preserved where the mixed layer depth is shallow ($\leq$5 cm) and sedimentation rates are higher than ~15 cm ka^{-1} [108].

Of the 68 sites included in this study, only 7 have sedimentation rates less than 15 cm ka^{-1} (Table 4) with coarse minimum sample resolutions between 350 and 1000 years (Figure 12 and Table 4). The 13 proxy records with the highest resolution come from sites with sedimentation rates ranging from 1.4 m ka^{-1} to 18.13 m ka^{-1}, where the depth and strength of climate signals are still modified within the sediment column but should preserve sub-millennial, centennial, and possibly sub-centennial variability.

4.3. Scope for Validation and Standardisation

Whilst the majority of diatom proxies covered in this review are based on ecological associations between the distribution of species in surface sediments and the mean oceanographic conditions above [10,70,71,81,82,94,100,109], validation (and/or calibration) against sea ice observations is problematic due to the relatively short 40-year instrumental record available for Antarctic sea ice, a timeframe that is not normally resolvable in marine sediment cores. Even at sites with exceptionally high sedimentation rates (>1 cm a^{-1}), signal attenuation from bioturbation and dating uncertainties may still preclude accurate alignment with satellite records. Where calibration is attempted across regions with decreasing (increasing) sea ice trends over recent decades [4], surface proxies may still predispose down-core records to underestimate (overestimate) past sea ice [97].

In addition to the limitations on validation, the diversity of existing records, in terms of the proxies, resolution, and age uncertainties, makes it particularly difficult to compare data and reconstructions. It is also possible, and perhaps likely, that a single 'standard' proxy cannot encapsulate the heterogenous nature of the sea ice environment. The current diversity of approaches may therefore be seen in a positive light, providing more detailed and meaningful descriptions of a greater number of sea ice-related variables. Additionally, these records are tailored to represent sea ice conditions in different locations. Without evaluating how well proxies work in different regions, it is difficult to assess the feasibility of a standard circum-Antarctic sea ice proxy. Also, given the divergent trends in sea ice seen in different sectors of Antarctica over recent decades [4], initial comparisons would probably be best applied to regions with similar sea ice history.

A potential first step towards validation and standardization would be to compare different proxies within a single core and a single proxy between different cores located within areas of similar sea ice history (Figure 10). Whilst the use of *Fragilariopsis curta* in the majority of sea ice proxies and regions (Figure 11) makes it a prime candidate for evaluation as a standard Antarctic sea ice proxy, the analytical efficiency afforded by the relatively new HBIs also warrants further development to hone its ecological association with sea ice.

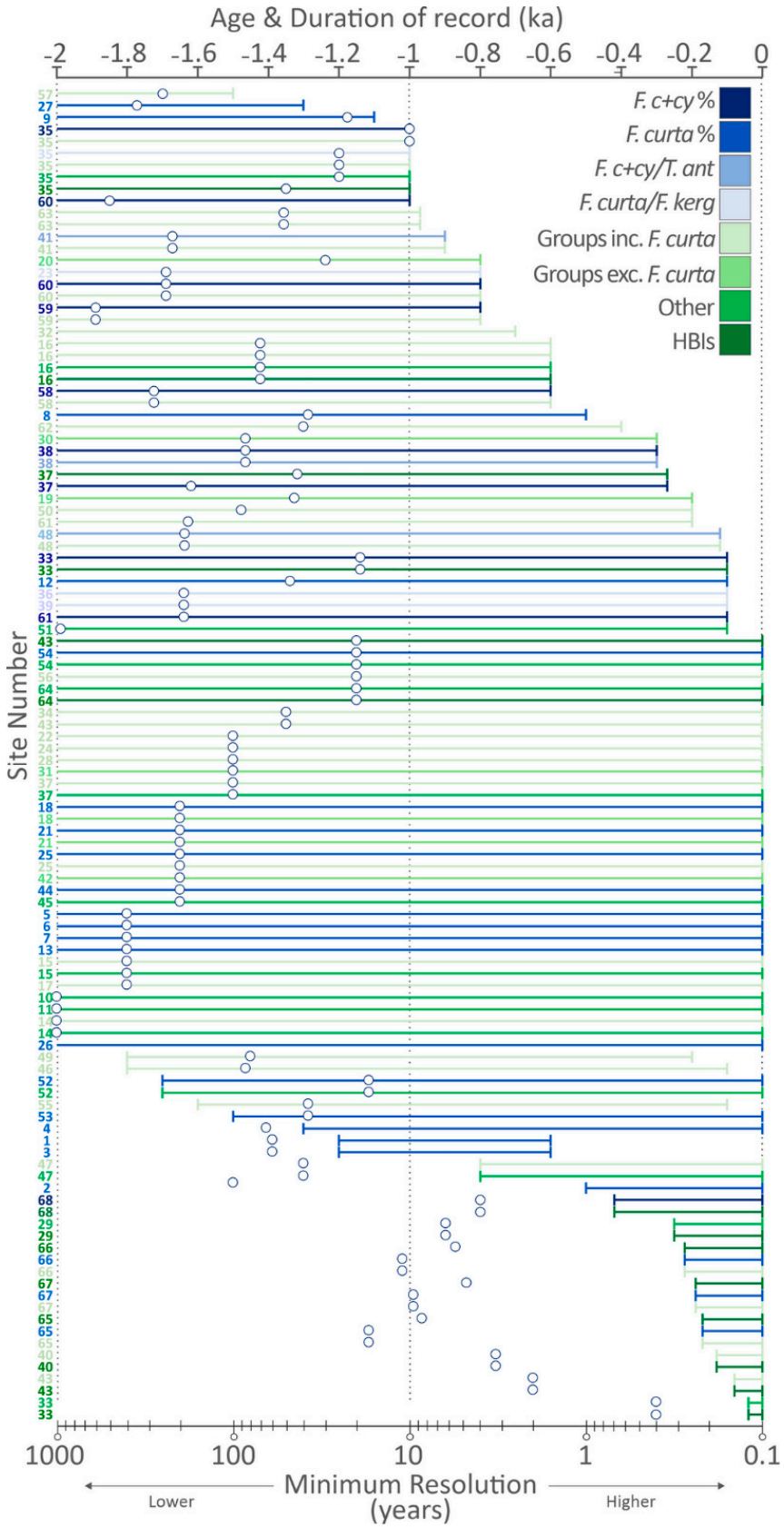

Figure 12. Plot showing the age, duration (horizontal lines, upper axis), and minimum resolution (open circles, bottom axis) for all downcore proxy records (site numbers, left axis) of sea ice included in this review.

5. Conclusions

This review provides a thorough evaluation of the diatom-based proxies used to reconstruct Antarctic sea ice of the past 2 ka. The study collates 112 records from 68 core sites, with proxies based on more than 30 different combinations of diatom taxa as well as HBI biomarkers. Presenting the origins and tenets of the proxies indicates how their varied composition reflects the ecological and taxonomic diversity of the sea ice environment. The wide variety of diatom-based sea ice proxies may limit the opportunities and complicate data assimilation and proxy standardisation but this diversity also suggests that one 'standard' diatom-based proxy is probably not appropriate for the varied ecological conditions of Antarctic sea ice. The broad range of proxies currently available can provide richer, localized perspective, and therefore potential for a more detailed insight into the different ways that sea ice conditions have changed in the past.

The detailed inventory of proxies and cores presented within this review provides a valuable resource for future research since it summarizes essential reference data on 112 existing sea ice records into a single, readily accessible publication. This resource will permit easy identification of: where records with certain time frames and/or resolutions occur; where specific proxies are applied; where comparisons between proxies and records are feasible; and where suitable records for regional syntheses occur. Mapping the distribution of records also emphasizes the large areas of continental shelf with sparse or no records of past sea ice. This review of existing records will hopefully encourage more informed decisions on the choice of proxy and temporal framework, ultimately leading to greater compatibility and consistency in the diatom-based reconstructions of Antarctic sea ice.

Author Contributions: Conceptualisation: C.S.A.; Outline and approach: C.S.A.; Investigation & resources: C.S.A. and Z.C.W.; Writing: C.S.A. and Z.C.W.; Reviewing and editing: C.S.A. and Z.C.W.; Corrections and proof reading: C.S.A. and Z.C.W. All authors have read and agreed to the published version of the manuscript.

Funding: This research was funded by British Antarctic Survey, with core funding from the Natural Environment Research Council and a PhD studentship from the National Environments Research Council Great Western 4+ Doctoral Training Partnership.

Data Availability Statement: Not applicable.

Acknowledgments: This work forms part of the British Antarctic Survey programme 'Polar Science for Planet Earth' and is a contribution to the PAGES 2k Network (through the CLIVASH2k project). Past Global Changes (PAGES) is supported by the US National Science Foundation and the Swiss Academy of Sciences. We thank Liz Thomas for her support in producing this review and we are grateful to the two anonymous reviewers for their constructive comments and suggestions which helped to improve the quality of the manuscript.

Conflicts of Interest: The authors declare no conflict of interest.

Appendix A

Information on diatom taxa included in Antarctic sea ice proxies:

1. *Fragilariopsis curta* is closely associated with sea ice throughout the Southern Ocean. *F. curta* is a common component of the diatom assemblage within the sea ice environment (often as a dominant species) in sea ice, in ice edge blooms, and in waters close to the sea ice [103,110–119]. This sea ice association is supported by plankton and sediment trap samples that show the distribution of *F. curta* to be broadly confined by the northern limit of sea ice [120,121]. In surface sediments, *F. curta* abundances increase southwards from the maximum limit of seasonal sea ice [81,82]. High abundances (>20%) are found in areas where summer sea surface temperatures (SSSTs) are below 0.5 °C [82] and where seasonal sea ice persists for 9–11 months/year [81]. The highest recorded sedimentary abundances (>60%) occur in the Ross Sea, Prydz Bay, and the Weddell Sea [12,81].

2. *Fragilariopsis cylindrus* is found in a range of sea ice settings and in waters closely influenced by sea ice, where they often occur as the dominant species [103,110–114,116,118,121,122]. Whilst

widely accepted as a sea ice-related diatom, *F. cylindrus* has also been associated with melt waters and stratified conditions [31,49,104,111], especially in the Ross Sea [11,123]. In surface sediments, *F. cylindrus* abundances of >10% are found where SSSTs are below −0.5 °C and sea ice is present for 3–10 months/year [81,82,124].

3. *Thalassiosira antarctica* is not usually found in sea ice but is recognized as a sea ice associated diatom, living in waters adjacent to sea ice, in crack pools, and in waters with unconsolidated sea ice [110,112,119,123,125]. The highest abundances in the Ross Sea are found near to the coast and may indicate a link with ice shelf and tidewater glaciers [123]. The occurrence of *T. antarctica* in sediment traps and seasonally laminated diatomaceous sediments supports the assertion that *T. antarctica* is primarily a member of the late summer and/or autumn phytoplankton community [12,32,106,126]. The distribution of *T. antarctica* in surface sediments is broadly consistent with its occurrence in surface waters. The highest abundances (>25%) are typically observed in coastal regions that experience >6 months sea ice per year and have summer SSTs between −1 and 0 °C [13,81,82,123].

4. *Fragilariopsis sublinearis* follows a similar distribution to *F. obliquecostata* in surface waters. The highest abundances (5–10%) of *F. sublinearis* are located almost exclusively in Prydz Bay, the Ross Sea, the Weddell Sea, and along the Wilkes Land margin, close to and within the maximum February sea ice extent [71,112,120,127]. In sediments, relative abundances of *F. sublinearis* above 2% occur in locations where sea ice is present for >7.5 months/year [70,81,82].

5. *Fragilariopsis kerguelensis* is an endemic Southern Ocean, and pelagic marine diatom is common in the iron-limited waters of the Antarctic Circumpolar Current with peak productivity along the southern boundary of the Polar Front [128–131]. Experiments and observations show that the optimal growth of *F. kerguelensis* occurs in 4–5 °C waters—the range of summer sea surface temperatures in the Polar Front Zone [131,132]. In surface sediments, *F. kerguelensis* dominates diatom assemblages in the Antarctic and Polar Front Zone throughout most of the Southern Ocean [129–131] and is negatively correlated with sea ice concentrations [133].

6. *Fragilariopsis obliquecostata* is also associated with sea ice but is less common and typically confined to more southerly locations than either *F. curta* or *F. cylindrus*. *F. obliquecostata* has been recorded in pack ice, land fast ice, and within waters of the marginal ice zone of the Weddell and Amundsen Seas [110,112,114]. In surface sediments, *F. obliquecostata* is less abundant than *F. cylindrus* with elevated abundances of >5% generally found south of the Antarctic Divergence where SSSTs are below 0 °C [70,82]. Elevated abundances of *F. obliquecostata* in the sediments broadly correspond to the area of maximum perennial sea ice and/or locations that experience >7 m/y sea ice cover [81] with the highest abundances of >10% recorded off the Victoria Land coast in the Ross Sea, in the Weddell Sea, and in the Prydz Bay region [82,123].

7. *Fragilariopsis rhombica* is associated with regions close to the Antarctic coast and ice shelves [44,134]. Although it has been recorded in sea ice samples, *F. rhombica* is absent from descriptions of common sea ice taxa and is more abundant in the waters immediately north of the sea ice edge [110,116,135]. *F. rhombica*'s distribution in surface sediments is linked with the Antarctic Zone with maximum relative abundances of >10% found in areas where summer sea surface temperatures range from −1.5 to 1 °C and sea ice cover persists for 7–9 months of the year [81,82,124].

8. *Fragilariopsis ritscheri* is an endemic Antarctic species that is usually found at lower abundances than other *Fragilariopsis* species [82,120]. In sediments, *F. ritscheri* is recorded at highest abundances of 1.5–3% where surface water temperatures range between −2.0 and 1 °C, broadly consistent with the area south of the average winter sea ice extent [81,82,136].

9. *Fragilariopsis vanheurckii* is generally considered a sea ice diatom [135,137,138], and is also commonly found in waters close to the sea ice edge and in the stratified melt waters following sea ice melt [111,114]. Analyses of the diatom assemblage in sediment trap material from the northwest Weddell Sea showed that *F. vanheurckii* comprised the highest abundances of >15% when the sea ice edge was at or in close proximity to the mooring

site [71]. In sediment assemblages, the highest abundances of >8% *F. vanheurckii* have been recorded in the Amundsen Sea [114] and northeast Antarctic Peninsula [139].

10. *Actinocyclus actinochilus* is linked with cool waters. In surface sediments, the distribution of *A. actinochilus* relates to surface water temperatures between −2 and 2 °C, broadly equivalent to the region between the minimum and maximum ice cover [81,82]. The highest abundances of *A. actinochilus* are reported from sediments in the Amundsen Sea (up to 14.4%, [114]) and Enderby Basin (9.38–13.33%, [131]). In other regions, *A. actinochilus* is more commonly present at abundances between 1 and 3% [20,81,82,123,140].

11. *Porosira glacialis* is a bipolar diatom species associated with cold shelf waters adjacent to sea ice [81,82]. *P. glacialis* is purported to grow in the open ocean beyond the perennial sea ice edge [81,82], and, while *P. glacialis* has been observed in waters with high concentrations of slush and wave-exposed shore ice, it has not been found in sea ice [110,125,141]. In sediments, *P. glacialis* is located shoreward of the maximum winter sea ice extent and reaches maximum abundances (>2%) beneath regions with February SSTs ranging from 0 to 0.5 °C [81] and at least 7.5 months per year sea ice cover [20,81]. While *P. glacialis* usually comprises only a minor component of the diatom assemblage, there are several records of diatomaceous laminae in which *P. glacialis* is visually one of the most noticeable taxa in late summer/autumn laminae from the Dumont d'Urville Trough, Mertz Ninnis Trough [32,142], Iceberg Alley [28], and the MacRobertson Shelf [106].

12. *Entomoneis kjellmanii* is a common member of the spring bottom ice community (particularly fast ice) prior to ice break out [74,143–146]. It is rarely observed in other sea ice habitats or in the surrounding waters, presenting a particularly robust affiliation with early spring, coastal sea ice conditions.

13. *Navicula glaceii* is a cryophilic, neritic diatom [141,147]. *N. glaceii* is particularly associated with the 'slushy' semi-frozen tideline habitat in fast ice and may be abundant in adjacent waters where it is seeded from melting and/or fragmentation of sea ice in the nearshore area [148].

14 and 15. *Nitzschia stellata* and *Berkeleya adeliensis* are categorized as 'tube dwelling" sympagic diatoms, frequently reported in fast ice samples from coastal regions of Antarctica, particularly East Antarctica [117,149–152]. Both *N. stellata* and *B. adeliensis* can be dominant species within the sea ice, but are only rarely found in the adjacent waters or underlying sediments [115,149,153,154].

16. *Thalassiosira australis* is found in and around sea ice and can form dense mats on the underside of fast ice in coastal areas of East Antarctica [144,155–157]. *T. australis* resting spores are also found in sediments under fast ice and in sediments from seasonally open water sites closely 'downstream' of fast ice [158].

17. *Pleurosigma directum* is a planktic pennate species found at low (rare) abundances in many regions and described as "probably cosmopolitan" [159].

18. *Pinnularia quadratarea* is a pennate benthic species, found within and on congelation and fast ice. *P. quadraterea* is more heavily silicified and dissolution-resistant than many other sympagic diatoms, and, as such, is often present within the underlying sediments [44,153,160].

19. *Fragilaria striulata* is a marine species of this predominantly freshwater genus, widely distributed throughout the North Atlantic and Arctic Oceans. Mostly recorded as a benthic and epiphytic littoral species, it has also been reported as a neritic planktonic species [159,161]. In the Southern Hemisphere, *F. striulata* has been found in waters and surface sediments along the Chilean coast and at nearshore sites in Antarctica [161–163].

20. *Synedropsis* is an araphid bi-polar genus associated with sea ice. In the Antarctic, it is found predominantly within the bottom ice community or as an epiphyte on other diatoms [164,165].

References

1. Fetterer, F.; Knowles, K.; Meier, W.N.; Savoie, M.; Windnagel, A.K. *Sea Ice Index, Version 3 (Southern Hemisphere)*; National Snow and Ice Data Center: Boulder, CO, USA, 2017.
2. Stammerjohn, S.; Massom, R.; Rind, D.; Martinson, D. Regions of rapid sea ice change: An inter-hemispheric seasonal comparison. *Geophys. Res. Lett.* **2012**, *39*, L06501. [CrossRef]
3. Holland, P.R. The seasonality of Antarctic sea ice trends. *Geophys. Res. Lett.* **2014**, *41*, 4230–4237. [CrossRef]
4. Parkinson, C.L. A 40-y record reveals gradual Antarctic sea ice increases followed by decreases at rates far exceeding the rates seen in the Arctic. *Proc. Natl. Acad. Sci. USA* **2019**, *116*, 14414–14423. [CrossRef]
5. Parkinson, C.L.; Cavalieri, D.J. Antarctic sea ice variability and trends, 1979–2010. *Cryosphere* **2012**, *6*, 871–880. [CrossRef]
6. Rosenblum, E.; Eisenman, I. Sea Ice Trends in Climate Models Only Accurate in Runs with Biased Global Warming. *J. Clim.* **2017**, *30*, 6265–6278. [CrossRef]
7. Fox-Kemper, B.; Hewitt, H.T.; Xiao, C.; Aðalgeirsdóttir, G.; Drijfhout, S.S.; Edwards, T.L.; Golledge, N.R.; Hemer, M.; Kopp, R.E.; Krinner, G.; et al. Ocean, Cryosphere and Sea Level Change. In *Climate Change 2021: The Physical Science Basis. Contribution of Working Group I to the Sixth Assessment Report of the Intergovernmental Panel on Climate Change*; Masson Delmotte, V., Zhai, P., Pirani, A., Connors, S.L., Péan, C., Berger, S., Caud, N., Chen, Y., Goldfarb, L., Gomis, M.I., et al., Eds.; Cambridge University Press: Cambridge, UK, 2021.
8. Thomas, E.R.; Allen, C.S.; Etourneau, J.; King, A.C.F.; Severi, M.; Winton, V.H.L.; Müller, J.; Crosta, X.; Peck, V.L. Antarctic Sea Ice Proxies from Marine and Ice Core Archives Suitable for Reconstructing Sea Ice over the past 2000 Years. *Geosciences* **2019**, *9*, 509. [CrossRef]
9. Zonneveld, K.A.F.; Versteegh, G.J.M.; Kasten, S.; Eglinton, T.I.; Emeis, K.C.; Huguet, C.; Koch, B.P.; de Lange, G.J.; de Leeuw, J.W.; Middelburg, J.J.; et al. Selective preservation of organic matter in marine environments; processes and impact on the sedimentary record. *Biogeosciences* **2010**, *7*, 483–511. [CrossRef]
10. Belt, S.T.; Smik, L.; Brown, T.A.; Kim, J.H.; Rowland, S.J.; Allen, C.S.; Gal, J.K.; Shin, K.H.; Lee, J.I.; Taylor, K.W.R. Source identification and distribution reveals the potential of the geochemical Antarctic sea ice proxy IPSO25. *Nat. Commun.* **2016**, *7*, 12655. [CrossRef]
11. Leventer, A.; Dunbar, R.B.; DeMaster, D.J. Diatom Evidence for Late Holocene Climatic Events in Granite Harbor, Antarctica. *Paleoceanography* **1993**, *8*, 373–386. [CrossRef]
12. Leventer, A.; Dunbar, R.B. Recent Diatom Record of McMurdo Sound, Antarctica: Implications for History of Sea Ice Extent. *Paleoceanography* **1988**, *3*, 259–274. [CrossRef]
13. Cunningham, W.L.; Leventer, A.; Andrews, J.T.; Jennings, A.E.; Licht, K. Late Pleistocene-Holocene marine condtions in the Ross Sea, Antarctica: Evidence from the diatom record. *Holocene* **1999**, *9*, 129–139. [CrossRef]
14. Mezgec, K.; Stenni, B.; Crosta, X.; Masson-Delmotte, V.; Baroni, C.; Braida, M.; Ciardini, V.; Colizza, E.; Melis, R.; Salvatore, M.C.; et al. Holocene sea ice variability driven by wind and polynya efficiency in the Ross Sea. *Nat. Commun.* **2017**, *8*, 1334. [CrossRef]
15. Minzoni, R.T.; Majewski, W.; Anderson, J.B.; Yokoyama, Y.; Fernandez, R.; Jakobsson, M. Oceanographic influences on the stability of the Cosgrove Ice Shelf, Antarctica. *Holocene* **2017**, *27*, 1645–1658. [CrossRef]
16. Hemer, M.A.; Harris, P.T. Sediment core from beneath the Amery Ice Shelf, East Antarctica, suggests mid-Holocene ice-shelf retreat. *Geology* **2003**, *31*, 127–130. [CrossRef]
17. Berg, S.; Wagner, B.; Cremer, H.; Leng, M.; Melles, M. Late Quaternary environmental and climate history of Rauer Group, East Antarctica. *Palaeogeogr. Palaeoclimatol. Palaeoecol.* **2010**, *297*, 201–213. [CrossRef]
18. Crosta, X.; Crespin, J.; Swingedouw, D.; Marti, O.; Masson-Delmotte, V.; Etourneau, J.; Goosse, H.; Braconnot, P.; Yam, R.; Brailovski, I.; et al. Ocean as the main driver of Antarctic ice sheet retreat during the Holocene. *Glob. Planet. Change* **2018**, *166*, 62–74. [CrossRef]
19. Denis, D.; Crosta, X.; Barbara, L.; Massé, G.; Renssen, H.; Ther, O.; Giraudeau, J. Sea ice and wind variability during the Holocene in East Antarctica: Insight on middle–high latitude coupling. *Quat. Sci. Rev.* **2010**, *29*, 3709–3719. [CrossRef]
20. Pike, J.; Crosta, X.; Maddison, E.J.; Stickley, C.E.; Denis, D.; Barbara, L.; Renssen, H. Observations on the relationship between the Antarctic coastal diatoms *Thalassiosira antarctica* Comber and *Porosira glacialis* (Grunow) Jørgensen and sea ice concentrations during the late Quaternary. *Mar. Micropaleontol.* **2009**, *73*, 14–25. [CrossRef]
21. Taylor, F.; McMinn, A. Late Quaternary Diatom Assemblages from Prydz Bay, Eastern Antarctica. *Quat. Res.* **2002**, *57*, 151–161. [CrossRef]
22. McMinn, A. Late Holocene increase in sea ice extent in fjords of the Vestfold Hills, eastern Antarctica. *Antarct. Sci.* **2000**, *12*, 80–88. [CrossRef]
23. McMinn, A.; Heijnis, H.; Harle, K.; McOrist, G. Late-Holocene climatic change recorded in sediment cores from Ellis Fjord, eastern Antarctica. *Holocene* **2001**, *11*, 291–300. [CrossRef]
24. Allen, C.S.; Oakes-Fretwell, L.M.; Anderson, J.B.; Hodgson, D.A. A record of Holocene glacial and oceanographic variability in Neny Fjord, Antarctic Peninsula. *Holocene* **2010**, *20*, 551–564. [CrossRef]
25. Peck, V.L.; Allen, C.S.; Kender, S.; McClymont, E.L.; Hodgson, D.A. Oceanographic variability on the West Antarctic Peninsula during the Holocene and the influence of upper circumpolar deep water. *Quat. Sci. Rev.* **2015**, *119*, 54–65. [CrossRef]

26. Taylor, F.; McMinn, A. Evidence from diatoms for Holocene climate fluctuation along the East Antarctic margin. *Holocene* **2001**, *11*, 455–466. [CrossRef]
27. Taylor, F.; Whitehead, J.; Domack, E. Holocene paleoclimate change in the Antarctic Peninsula: Evidence from the diatom, sedimentary and geochemical record. *Mar. Micropaleontol.* **2001**, *41*, 25–43. [CrossRef]
28. Alley, K.; Patacca, K.; Pike, J.; Dunbar, R.; Leventer, A. Iceberg Alley, East Antarctic Margin: Continuously laminated diatomaceous sediments from the late Holocene. *Mar. Micropaleontol.* **2018**, *140*, 56–68. [CrossRef]
29. Rathburn, A.E.; Pichon, J.J.; Ayress, M.A.; DeDeckker, P. Microfossil and stable-isotope evidence for changes in Late Holocene palaeoproductivity and palaeoceanographic conditions in the Prydz Bay region of Antarctica. *Palaeogeogr. Palaeoclimatol. Palaeoecol.* **1997**, *131*, 485–510. [CrossRef]
30. Campagne, P.; Crosta, X.; Houssais, M.N.; Swingedouw, D.; Schmidt, S.; Martin, A.; Devred, E.; Capo, S.; Marieu, V.; Closset, I.; et al. Glacial ice and atmospheric forcing on the Mertz Glacier Polynya over the past 250 years. *Nat. Commun.* **2015**, *6*, 6642. [CrossRef]
31. Cremer, H.; Gore, D.; Melles, M.; Roberts, D. Palaeoclimatic significance of late Quaternary diatom assemblages from southern Windmill Islands, East Antarctica. *Palaeogeogr. Palaeoclimatol. Palaeoecol.* **2003**, *195*, 261–280. [CrossRef]
32. Maddison, E.J.; Pike, J.; Dunbar, R. Seasonally laminated diatom-rich sediments from Dumont d'Urville Trough, East Antarctic Margin: Late-Holocene Neoglacial sea-ice conditions. *Holocene* **2012**, *22*, 857–875. [CrossRef]
33. Campagne, P.; Crosta, X.; Schmidt, S.; Noëlle Houssais, M.; Ther, O.; Massé, G. Sedimentary response to sea ice and atmospheric variability over the instrumental period off Adélie Land, East Antarctica. *Biogeosciences* **2016**, *13*, 4205–4218. [CrossRef]
34. Crosta, X.; Etourneau, J.; Orme, L.C.; Dalaiden, Q.; Campagne, P.; Swingedouw, D.; Goosse, H.; Massé, G.; Miettinen, A.; McKay, R.M.; et al. Multi-decadal trends in Antarctic sea-ice extent driven by ENSO–SAM over the last 2000 years. *Nat. Geosci.* **2021**, *14*, 156–160. [CrossRef]
35. Kulbe, T.; Melles, M.; Verkulich, S.R.; Pushina, Z.V. East Antarctic Climate and Environmental Variability over the Last 9400 Years Inferred from Marine Sediments of the Bunger Oasis. *Arct. Antarct. Alp. Res.* **2001**, *33*, 223–230. [CrossRef]
36. Crosta, X.; Crespin, J.; Billy, I.; Ther, O. Major factors controlling Holocene delta C-13(org) changes in a seasonal sea-ice environment, Adelie Land, East Antarctica. *Glob. Biogeochem. Cycles* **2005**, *19*, 1–9. [CrossRef]
37. Crosta, X.; Debret, M.; Denis, D.; Courty, M.A.; Ther, O. Holocene long- and short-term climate changes off Adélie Land, East Antarctica. *Geochem. Geophys. Geosystems* **2007**, *8*, Q11009. [CrossRef]
38. Crosta, X.; Denis, D.; Ther, O. Sea ice seasonality during the Holocene, Adelie Land, East Antarctica. *Mar. Micropaleontol.* **2008**, *66*, 222–232. [CrossRef]
39. Denis, D.; Crosta, X.; Schmidt, S.; Carson, D.S.; Ganeshram, R.S.; Renssen, H.; Bout-Roumazeilles, V.; Zaragosi, S.; Martin, B.; Cremer, M.; et al. Holocene glacier and deep water dynamics, Adélie Land region, East Antarctica. *Quat. Sci. Rev.* **2009**, *28*, 1291–1303. [CrossRef]
40. Kim, S.; Yoo, K.-C.; Lee, J.I.; Khim, B.-K.; Bak, Y.-S.; Lee, M.K.; Lee, J.; Domack, E.W.; Christ, A.J.; Yoon, H.I. Holocene paleoceanography of Bigo Bay, west Antarctic Peninsula: Connections between surface water productivity and nutrient utilization and its implication for surface-deep water mass exchange. *Quat. Sci. Rev.* **2018**, *192*, 59–70. [CrossRef]
41. Etourneau, J.; Collins, L.G.; Willmott, V.; Kim, J.H.; Barbara, L.; Leventer, A.; Schouten, S.; Sinninghe Damsté, J.S.; Bianchini, A.; Klein, V.; et al. Holocene climate variations in the western Antarctic Peninsula: Evidence for sea ice extent predominantly controlled by changes in insolation and ENSO variability. *Clim. Past* **2013**, *9*, 1431–1446. [CrossRef]
42. Sjunneskog, C.; Taylor, F. Postglacial marine diatom record of the Palmer Deep, Antarctic Peninsula (ODP Leg 178, Site 1098) 1. Total diatom abundance. *Paleoceanography* **2002**, *17*, PAL-4. [CrossRef]
43. Taylor, F.; Sjunneskog, C. Postglacial marine diatom record of the Palmer Deep, Antarctic Peninsula (ODP Leg 178, Site 1098) 2. Diatom assemblages. *Paleoceanography* **2002**, *17*, PAL-2. [CrossRef]
44. Leventer, A. The Fate of Antarctic "Sea-ice diatoms" and their use as palaeoenvironmental indicators. In *Antarctic Sea Ice Biological, Processes, Interactions and Variability*; Union, A.G., Ed.; American Geophysical Union: Washington, DC, USA, 1998; pp. 121–137.
45. Leventer, A.; Domack, E.W.; Ishman, S.E.; Brachfeld, S.; McClennen, C.E.; Manley, P. Productivity cycles of 200–300 years in the Antarctic Peninsula region: Understanding linkages among the sun, atmosphere, oceans, sea ice, and biota. *Geol. Soc. Am. Bull.* **1996**, *108*, 1626–1644. [CrossRef]
46. Roberts, S.J.; Monien, P.; Foster, L.C.; Loftfield, J.; Hocking, E.P.; Schnetger, B.; Pearson, E.J.; Juggins, S.; Fretwell, P.; Ireland, L.; et al. Past penguin colony responses to explosive volcanism on the Antarctic Peninsula. *Nat. Commun.* **2017**, *8*, 14914. [CrossRef] [PubMed]
47. Barbara, L.; Crosta, X.; Schmidt, S.; Masse, G. Diatoms and biomarkers evidence for major changes in sea ice conditions prior the instrumental period in Antarctic Peninsula. *Quat. Sci. Rev.* **2013**, *79*, 99–110. [CrossRef]
48. Yoon, H.I.; Park, B.-K.; Kim, Y.; Kang, C.Y. Glaciomarine sedimentation and its paleoclimatic implications on the Antarctic Peninsula shelf over the last 15,000 years. *Palaeogeogr. Palaeoclimatol. Palaeoecol.* **2002**, *185*, 235–254. [CrossRef]
49. Minzoni, R.T.; Anderson, J.B.; Fernandez, R.; Wellner, J.S. Marine record of Holocene climate, ocean, and cryosphere interactions: Herbert Sound, James Ross Island, Antarctica. *Quat. Sci. Rev.* **2015**, *129*, 239–259. [CrossRef]
50. Barbara, L.; Crosta, X.; Leventer, A.; Schmidt, S.; Etourneau, J.; Domack, E.; Masse, G. Environmental responses of the Northeast Antarctic Peninsula to the Holocene climate variability. *Paleoceanography* **2016**, *31*, 131–147. [CrossRef]

51. Heroy, D.C.; Sjunneskog, C.; Anderson, J.B. Holocene climate change in the Bransfield Basin, Antarctic Peninsula: Evidence from sediment and diatom analysis. *Antarct. Sci.* **2008**, *20*, 69–87. [CrossRef]
52. Michalchuk, B.R.; Anderson, J.B.; Wellner, J.S.; Manley, P.L.; Majewski, W.; Bohaty, S. Holocene climate and glacial history of the northeastern Antarctic Peninsula: The marine sedimentary record from a long SHALDRIL core. *Quat. Sci. Rev.* **2009**, *28*, 3049–3065. [CrossRef]
53. Barcena, M.A.; Fabres, B.; Isla, E.; Flores, J.A.; Sierro, F.J.; Canals, M.; Palanques, A. Holocene neoglacial events in the Bransfield Strait (Antarctica). Palaeocenographic and palaeoclimatic significance. *Sci. Mar.* **2006**, *70*, 607–619. [CrossRef]
54. Barcena, M.A.; Isla, E.; Plaza, A.; Flores, J.A.; Sierro, F.J.; Masque, P.; Sanchez-Cabeza, J.A.; Palanques, A. Bioaccumulation record and paleoclimatic significance in the Western Bransfield Strait. The last 2000 years. *Deep-Sea Res. Part Ii-Top. Stud. Oceanogr.* **2002**, *49*, 935–950. [CrossRef]
55. Kyrmanidou, A.; Vadman, K.J.; Ishman, S.E.; Leventer, A.; Brachfeld, S.; Domack, E.W.; Wellner, J.S. Late Holocene oceanographic and climatic variability recorded by the Perseverance Drift, northwestern Weddell Sea, based on benthic foraminifera and diatoms. *Mar. Micropaleontol.* **2018**, *141*, 10–22. [CrossRef]
56. Barcena, M.A.; Gersonde, R.; Ledesma, S.; Fabres, J.; Calafat, A.M.; Canals, M.; Sierro, F.J.; Flores, J.A. Record of Holocene glacial oscillations in Bransfield Basin as revealed by siliceous microfossil assemblages. *Antarct. Sci.* **1998**, *10*, 269–285. [CrossRef]
57. Milliken, K.T.; Anderson, J.B.; Wellner, J.S.; Bohaty, S.M.; Manley, P.L. High-resolution Holocene climate record from Maxwell Bay, South Shetland Islands, Antarctica. *Geol. Soc. Am. Bull.* **2009**, *121*, 1711–1725. [CrossRef]
58. Yoon, H.I.; Yoo, K.C.; Park, B.K.; Kim, Y.; Khim, B.K.; Kang, C.Y. The origin of massive diamicton in Marian and Potter coves, King George Island, West Antarctica. *Geosci. J.* **2004**, *8*, 1–10. [CrossRef]
59. Yoo, K.-C.; Yoon, H.I.; Kim, J.-K.; Khim, B.-K. Sedimentological, geochemical and palaeontological evidence for a neoglacial cold event during the late Holocene in the continental shelf of the northern South Shetland Islands, West Antarctica. *Polar Res.* **2009**, *28*, 177–192. [CrossRef]
60. Yoon, H.I.; Yoo, K.C.; Bak, Y.S.; Lim, H.S.; Kim, Y.; Lee, J.I. Late Holocene cyclic glaciomarine sedimentation in a subpolar fjord of the South Shetland Islands, Antarctica, and its paleoceanographic significance: Sedimentological, geochemical, and paleontological evidence. *Geol. Soc. Am. Bull.* **2010**, *122*, 1298–1307. [CrossRef]
61. Divine, D.V.; Koç, N.; Isaksson, E.; Nielsen, S.; Crosta, X.; Godtliebsen, F. Holocene Antarctic climate variability from ice and marine sediment cores: Insights on ocean-atmosphere interaction. *Quat. Sci. Rev.* **2010**, *29*, 303–312. [CrossRef]
62. Ferry, A.J.; Crosta, X.; Quilty, P.G.; Fink, D.; Howard, W.; Armand, L.K. First records of winter sea ice concentration in the southwest Pacific sector of the Southern Ocean. *Paleoceanography* **2015**, *30*, 1525–1539. [CrossRef]
63. Xiao, W.S.; Esper, O.; Gersonde, R. Last Glacial-Holocene climate variability in the Atlantic sector of the Southern Ocean. *Quat. Sci. Rev.* **2016**, *135*, 115–137. [CrossRef]
64. Bianchi, C.; Gersonde, R. Climate evolution at the last deglaciation: The role of the Southern Ocean. *Earth Planet. Sci. Lett.* **2004**, *228*, 407–424. [CrossRef]
65. Orme, L.C.; Crosta, X.; Miettinen, A.; Divine, D.V.; Husum, K.; Isaksson, E.; Wacker, L.; Mohan, R.; Ther, O.; Ikehara, M. Sea surface temperature in the Indian sector of the Southern Ocean over the Late Glacial and Holocene. *Clim. Past* **2020**, *16*, 1451–1467. [CrossRef]
66. Tesi, T.; Belt, S.T.; Gariboldi, K.; Muschitiello, F.; Smik, L.; Finocchiaro, F.; Giglio, F.; Colizza, E.; Gazzurra, G.; Giordano, P.; et al. Resolving sea ice dynamics in the north-western Ross Sea during the last 2.6 ka: From seasonal to millennial timescales. *Quat. Sci. Rev.* **2020**, *237*, 106299. [CrossRef]
67. Vorrath, M.E.; Müller, J.; Rebolledo, L.; Cárdenas, P.; Shi, X.; Esper, O.; Opel, T.; Geibert, W.; Muñoz, P.; Haas, C.; et al. Sea ice dynamics in the Bransfield Strait, Antarctic Peninsula, during the past 240 years: A multi-proxy intercomparison study. *Clim. Past* **2020**, *16*, 2459–2483. [CrossRef]
68. Ashley, K.E.; Crosta, X.; Etourneau, J.; Campagne, P.; Gilchrist, H.; Ibraheem, U.; Greene, S.E.; Schmidt, S.; Eley, Y.; Massé, G.; et al. Exploring the use of compound-specific carbon isotopes as a palaeoproductivity proxy off the coast of Adélie Land, East Antarctica. *Biogeosciences* **2021**, *18*, 5555–5571. [CrossRef]
69. Hogg, A.G.; Heaton, T.J.; Hua, Q.; Palmer, J.G.; Turney, C.S.M.; Southon, J.; Bayliss, A.; Blackwell, P.G.; Boswijk, G.; Bronk Ramsey, C.; et al. SHCal20 Southern Hemisphere Calibration, 0–55,000 Years cal BP. *Radiocarbon* **2020**, *62*, 759–778. [CrossRef]
70. Esper, O.; Gersonde, R. New tools for the reconstruction of Pleistocene Antarctic sea ice. *Palaeogeogr. Palaeoclimatol. Palaeoecol.* **2014**, *399*, 260–283. [CrossRef]
71. Gersonde, R.; Zielinski, U. The reconstruction of late Quaternary Antarctic sea-ice distribution-the use of diatoms as a proxy for sea-ice. *Palaeogeogr. Palaeoclimatol. Palaeoecol.* **2000**, *162*, 263–286. [CrossRef]
72. Crosta, X.; Shukla, S.K.; Ther, O.; Ikehara, M.; Yamane, M.; Yokoyama, Y. Last Abundant Appearance Datum of Hemidiscus karstenii driven by climate change. *Mar. Micropaleontol.* **2020**, *157*, 101861. [CrossRef]
73. Crosta, X.; Sturm, A.; Armand, L.; Pichon, J.J. Late Quaternary sea ice history in the Indian sector of the Southern Ocean as recorded by diatom assemblages. *Mar. Micropaleontol.* **2004**, *50*, 209–223. [CrossRef]
74. Lazzara, L.; Nardello, I.; Ermanni, C.; Mangoni, O.; Saggiomo, V. Light environment and seasonal dynamics of microalgae in the annual sea ice at Terra Nova Bay, Ross Sea, Antarctica. *Antarct. Sci.* **2007**, *19*, 83–92. [CrossRef]
75. Perrin, R.A.; Lu, P.; Marchant, H.J. Seasonal variation in marine phytoplankton and ice algae at a shallow antarctic coastal site. *Hydrobiologia* **1987**, *146*, 33–46. [CrossRef]

76. Ryan, K.G.; Hegseth, E.N.; Martin, A.; Davy, S.K.; O'Toole, R.; Ralph, P.J.; McMinn, A.; Thorn, C.J. Comparison of the microalgal community within fast ice at two sites along the Ross Sea coast, Antarctica. *Antarct. Sci.* **2006**, *18*, 583–594. [CrossRef]
77. Kaczmarska, I.; Barbrick, N.E.; Ehrman, J.M.; Cant, G.P. *Eucampia* Index as an indicator of the Late Pleistocene oscillations of the winter sea-ice extent at the ODP Leg 119 Site 745B at the Kerguelen Plateau. *Hydrobiologia* **1993**, *269/270*, 103–112. [CrossRef]
78. Fryxell, G.A.; Prasad, A.K.S.K. *Eucampia antarctica* var. *recta* (Mangin) stat. nov. (*Biddulphiaceae, Bacillariophyceae*): Life stages at the Weddell Sea ice edge. *Phycologia* **1990**, *29*, 27–38. [CrossRef]
79. Allen, C.S. Proxy development: A new facet of morphological diversity in the marine diatom *Eucampia antarctica* (Castracane) Mangin. *J. Micropalaeontology* **2014**, *33*, 131–142. [CrossRef]
80. Leventer, A.; Domack, E.; Barkoukis, A.; McAndrews, B.; Murray, J. Laminations from the Palmer Deep: A diatom-based interpretation. *Paleoceanography* **2002**, *17*, 1–15. [CrossRef]
81. Armand, L.K.; Crosta, X.; Romero, O.; Pichon, J.-J. The biogeography of major diatom taxa in Southern Ocean sediments: 1. Sea ice related species. *Palaeogeogr. Palaeoclimatol. Palaeoecol.* **2005**, *223*, 93–126. [CrossRef]
82. Zielinski, U.; Gersonde, R. Diatom distribution in Southern Ocean surface sediments (Atlantic sector): Implications for palaeoenvironmental reconstructions. *Palaeogeogr. Palaeoclimatol. Palaeoecol.* **1997**, *129*, 213–250. [CrossRef]
83. Świło, M.; Majewski, W.; Minzoni, R.T.; Anderson, J.B. Diatom assemblages from coastal settings of West Antarctica. *Mar. Micropaleontol.* **2016**, *125*, 95–109. [CrossRef]
84. Crosta, X.; Pichon, J.; Labracherie, M. Distribution of *Chaetoceros* resting spores in modern peri-Antarctic sediments. *Mar. Micropaleontol.* **1997**, *29*, 283–299. [CrossRef]
85. Belt, S.T.; Masse, G.; Rowland, S.J.; Poulin, M.; Michel, C.; LeBlanc, B. A novel chemical fossil of palaeo sea ice: IP25. *Org. Geochem.* **2007**, *38*, 16–27. [CrossRef]
86. Brown, T.A.; Belt, S.T.; Tatarek, A.; Mundy, C.J. Source identification of the Arctic sea ice proxy IP25. *Nat. Commun.* **2014**, *5*, 4197. [CrossRef] [PubMed]
87. Cabedo-Sanz, P.; Belt, S.T.; Knies, J.; Husum, K. Identification of contrasting seasonal sea ice conditions during the Younger Dryas. *Quat. Sci. Rev.* **2013**, *79*, 74–86. [CrossRef]
88. Fahl, K.; Stein, R. Modern seasonal variability and deglacial/Holocene change of central Arctic Ocean sea-ice cover: New insights from biomarker proxy records. *Earth Planet. Sci. Lett.* **2012**, *351*, 123–133. [CrossRef]
89. Xiao, X.; Fahl, K.; Stein, R. Biomarker distributions in surface sediments from the Kara and Laptev seas (Arctic Ocean): Indicators for organic-carbon sources and sea-ice coverage. *Quat. Sci. Rev.* **2013**, *79*, 40–52. [CrossRef]
90. Massé, G.; Rowland, S.J.; Sicre, M.A.; Jacob, J.; Jansen, E.; Belt, S.T. Abrupt climate changes for Iceland during the last millennium: Evidence from high resolution sea ice reconstructions. *Earth Planet. Sci. Lett.* **2008**, *269*, 565–569. [CrossRef]
91. Barbara, L.; Crosta, X.; Massé, G.; Ther, O. Deglacial environments in eastern Prydz Bay, East Antarctica. *Quat. Sci. Rev.* **2010**, *29*, 2731–2740. [CrossRef]
92. Cárdenas, P.; Lange, C.B.; Vernet, M.; Esper, O.; Srain, B.; Vorrath, M.-E.; Ehrhardt, S.; Müller, J.; Kuhn, G.; Arz, H.W.; et al. Biogeochemical proxies and diatoms in surface sediments across the Drake Passage reflect oceanic domains and frontal systems in the region. *Prog. Oceanogr.* **2018**, *174*, 72–88. [CrossRef]
93. Collins, L.G.; Allen, C.S.; Pike, J.; Hodgson, D.A.; Weckström, K.; Massé, G. Evaluating highly branched isoprenoid (HBI) biomarkers as a novel Antarctic sea-ice proxy in deep ocean glacial age sediments. *Quat. Sci. Rev.* **2013**, *79*, 87–98. [CrossRef]
94. Massé, G.; Belt, S.T.; Crosta, X.; Schmidt, S.; Snape, I.; Thomas, D.N.; Rowland, S.J. Highly branched isoprenoids as proxies for variable sea ice conditions in the Southern Ocean. *Antarct. Sci.* **2011**, *23*, 487–498. [CrossRef]
95. Sinninghe Damsté, J.S.; Rijpstra, W.I.C.; Coolen, M.J.L.; Schouten, S.; Volkman, J.K. Rapid sulfurisation of highly branched isoprenoid (HBI) alkenes in sulfidic Holocene sediments from Ellis Fjord, Antarctica. *Org. Geochem.* **2007**, *38*, 128–139. [CrossRef]
96. Smik, L.; Belt, S.T.; Lieser, J.L.; Armand, L.K.; Leventer, A. Distributions of highly branched isoprenoid alkenes and other algal lipids in surface waters from East Antarctica: Further insights for biomarker-based paleo sea-ice reconstruction. *Org. Geochem.* **2016**, *95*, 71–80. [CrossRef]
97. Vorrath, M.E.; Muller, J.; Esper, O.; Mollenhauer, G.; Haas, C.; Schefuss, E.; Fahl, K. Highly branched isoprenoids for Southern Ocean sea ice reconstructions: A pilot study from the Western Antarctic Peninsula. *Biogeosciences* **2019**, *16*, 2961–2981. [CrossRef]
98. Belt, S.T. Source-specific biomarkers as proxies for Arctic and Antarctic sea ice. *Org. Geochem.* **2018**, *125*, 277–298. [CrossRef]
99. Allen, C.S.; Pike, J.; Pudsey, C.J.; Leventer, A. Submillennial variations in ocean conditions during deglaciation based on diatom assemblages from the southwest Atlantic. *Paleoceanography* **2005**, *20*, 16. [CrossRef]
100. Armand, L.; Ferry, A.J.; Leventer, A. Advances in palaeo sea ice estimation. In *Sea Ice*; Thomas, D.N., Ed.; John Wiley & Sons Ltd.: Chichester, UK, 2017; pp. 600–629.
101. Ferry, A.J.; Prvan, T.; Jersky, B.; Crosta, X.; Armand, L.K. Statistical modeling of southern ocean marine diatom proxy and winter sea ice data: Model comparison and developments. *Prog. Oceanogr.* **2015**, *131*, 100–112. [CrossRef]
102. Kang, S.H.; Fryxell, G.A. *Fragilariopsis cylindrus* (Grunow) Krieger-the most abundant diatom in water column assemblages of Antarctic marginal ice-edge zones. *Polar Biol.* **1992**, *12*, 609–627. [CrossRef]
103. Pike, J.; Allen, C.S.; Leventer, A.; Stickley, C.E.; Pudsey, C.J. Comparison of contemporary and fossil diatom assemblages from the western Antarctic Peninsula shelf. *Mar. Micropaleontol.* **2008**, *67*, 274–287. [CrossRef]
104. von Quillfeldt, C.H. The diatom *Fragilariopsis cylindrus* and its potential as an indicator species for cold water rather than for sea ice. *Vie Milieu* **2004**, *54*, 137–143.

105. Ashley, K.E.; McKay, R.; Etourneau, J.; Jimenez-Espejo, F.J.; Condron, A.; Albot, A.; Crosta, X.; Riesselman, C.; Seki, O.; Massé, G.; et al. Mid-Holocene Antarctic sea-ice increase driven by marine ice sheet retreat. *Clim. Past* **2021**, *17*, 1–19. [CrossRef]
106. Stickley, C.E.; Pike, J.; Leventer, A.; Dunbar, R.; Domack, E.W.; Brachfeld, S.; Manley, P.; McClennan, C. Deglacial ocean and climate seasonality in laminated diatom sediments, Mac.Robertson Shelf, Antarctica. *Palaeogeogr. Palaeoclimatol. Palaeoecol.* **2005**, *227*, 290–310. [CrossRef]
107. Anderson, D.M. Attenuation of millennial-scale events by bioturbation in marine sediments. *Paleoceanography* **2001**, *16*, 352–357. [CrossRef]
108. Liu, H.; Meyers, S.R.; Marcott, S.A. Unmixing deep-sea paleoclimate records: A study on bioturbation effects through convolution and deconvolution. *Earth Planet. Sci. Lett.* **2021**, *564*, 116883. [CrossRef]
109. Crosta, X.; Pichon, J.J.; Burckle, L.H. Application of modern analog technique to marine Antarctic diatoms: Reconstruction of maximum sea-ice extent at the Last Glacial Maximum. *Paleoceanography* **1998**, *13*, 284–297. [CrossRef]
110. Garrison, D.L. Antarctic Sea Ice Biota. *Am. Zool.* **1991**, *31*, 17–33. [CrossRef]
111. Hegseth, E.N.; Von Quillfeldt, C.H. Low phytoplankton biomass and ice algal blooms in the Weddell Sea during the ice-filled summer of 1997. *Antarct. Sci.* **2002**, *14*, 231–243. [CrossRef]
112. Kang, S.H.; Kang, J.S.; Lee, S.; Chung, K.H.; Kim, D.; Park, M.G. Antarctic phytoplankton assemblages in the marginal ice zone of the northwestern Weddell Sea. *J. Plankton Res.* **2001**, *23*, 333–352. [CrossRef]
113. Kang, S.-H.; Fryxell, G.A. Phytoplankton in the Weddell Sea, Antarctica: Composition, abundance and distribution in water-column assemblages of the marginal ice-edge zone during austral autumn. *Mar. Biol.* **1993**, *116*, 335–348. [CrossRef]
114. Kellogg, D.E.; Kellogg, T.B. Microfossil distributions in modern Amundsen Sea sediments. *Mar. Micropaleontol.* **1987**, *12*, 203–222. [CrossRef]
115. Leventer, A.; Dunbar, R. Diatom flux in McMurdo Sound, Antarctica. *Mar. Micropaleontol.* **1987**, *12*, 49–64. [CrossRef]
116. Ligowski, R.; Godlewski, M.; Lukowski, A. Sea ice diatoms and ice edge planktonic diatoms at the northern limit of the Weddell Sea pack ice. *Proc. NIPR Symp. Polar Biol.* **1992**, *5*, 9–20.
117. Saggiomo, M.; Poulin, M.; Mangoni, O.; Lazzara, L.; De Stefano, M.; Sarno, D.; Zingone, A. Spring-time dynamics of diatom communities in landfast and underlying platelet ice in Terra Nova Bay, Ross Sea, Antarctica. *J. Mar. Syst.* **2017**, *166*, 26–36. [CrossRef]
118. Schloss, I.; Estrada, M. Phytoplankton composition in the Weddell-Scotia Confluence area during austral spring in relation to hyrdrography. *Polar Biol.* **1994**, *14*, 77–90. [CrossRef]
119. Smetacek, V.; Scharek, R.; Gordon, L.I.; Eicken, H.; Fahrbach, E.; Rohardt, G.; Moore, S. Early spring phytoplankton blooms in ice platelet layers of the southern Weddell Sea, Antarctica. *Deep-Sea Res. Part A-Oceanogr. Res. Pap.* **1992**, *39*, 153–168. [CrossRef]
120. Cefarelli, A.O.; Ferrario, M.E.; Almandoz, G.O.; Atencío, A.G.; Akselman, R.; Vernet, M. Diversity of the diatom genus *Fragilariopsis* in the Argentine Sea and Antarctic waters: Morphology, distribution and abundance. *Polar Biol.* **2010**, *33*, 1463–1484. [CrossRef]
121. Rigual-Hernández, A.S.; Pilskaln, C.H.; Cortina, A.; Abrantes, F.; Armand, L.K. Diatom species fluxes in the seasonally ice-covered Antarctic Zone: New data from offshore Prydz Bay and comparison with other regions from the eastern Antarctic and western Pacific sectors of the Southern Ocean. *Deep Sea Res. Part II Top. Stud. Oceanogr.* **2019**, *161*, 92–104. [CrossRef]
122. Garrison, D.L.; Buck, C.E.; Fryxell, G. Algal assemblages in Antarctic pack ice and in ice-edge plankton. *J. Phycol.* **1987**, *23*, 564–572. [CrossRef]
123. Cunningham, W.L.; Leventer, A. Diatom assemblages in surface sediments of the Ross Sea: Relationship to present oceanographic conditions. *Antarct. Sci.* **1998**, *10*, 134–146. [CrossRef]
124. Leventer, A. Modern distribution of diatoms in sediments from the George-V-Coast, Antarctica. *Mar. Micropaleontol.* **1992**, *19*, 315–332. [CrossRef]
125. Gleitz, M.; Grossmann, S.; Scharek, R.; Smetacek, V. Ecology of diatom and bacterial assemblages in water associated with melting summer sea ice in the Weddell Sea, Antarctica. *Antarct. Sci.* **1996**, *8*, 135–146. [CrossRef]
126. Maddison, E.J.; Pike, J.; Leventer, A.; Domack, E.W. Deglacial seasonal and sub-seasonal diatom record from Palmer Deep, Antarctica. *J. Quat. Sci.* **2005**, *20*, 435–446. [CrossRef]
127. Garrison, D.L.; Jeffries, M.O.; Gibson, A.; Coale, S.L.; Neenan, D.; Fritsen, C.; Okolodkov, Y.B.; Gowing, M.M. Development of sea ice microbial communities during autumn ice formation in the Ross Sea. *Mar. Ecol. Prog. Ser.* **2003**, *259*, 1–15. [CrossRef]
128. Assmy, P.; Smetacek, V.; Montresor, M.; Klaas, C.; Henjes, J.; Strass, V.H.; Arrieta, J.M.; Bathmann, U.; Berg, G.M.; Breitbarth, E.; et al. Thick-shelled, grazer-protected diatoms decouple ocean carbon and silicon cycles in the iron-limited Antarctic Circumpolar Current. *Proc. Natl. Acad. Sci. USA* **2013**, *110*, 20633–20638. [CrossRef]
129. Bathmann, U.V.; Scharek, R.; Klaas, C.; Dubischar, C.D.; Smetacek, V. Spring development of phytoplankton biomass and composition in major water masses of the Atlantic sector of the Southern Ocean. *Deep-Sea Res. Part Ii-Top. Stud. Oceanogr.* **1997**, *44*, 51–67. [CrossRef]
130. Crosta, X.; Romero, O.; Armand, L.K.; Pichon, J.-J. The biogeography of major diatom taxa in Southern Ocean sediments: 2. Open ocean related species. *Palaeogeogr. Palaeoclimatol. Palaeoecol.* **2005**, *223*, 66–92. [CrossRef]
131. Mohan, R.; Quarshi, A.A.; Meloth, T.; Sudhakar, M. Diatoms from the surface waters of the Southern Ocean during the austral summer of 2004. *Curr. Sci.* **2011**, *100*, 1323–1327.

132. Fischer, G.; Gersonde, R.; Wefer, G. Organic carbon, biogenic silica and diatom fluxes in the marginal winter sea-ice zone and in the Polar Front Region: Interannual variations and differences in composition. *Deep-Sea Res. Part Ii-Top. Stud. Oceanogr.* **2002**, *49*, 1721–1745. [CrossRef]
133. Burckle, L.H.; Cirilli, J. Origin of diatom ooze belt in the Southern Ocean; implications for late Quaterary paleoceanography. *Micropaleontology* **1987**, *33*, 82–86. [CrossRef]
134. Mohan, R.; Shanvas, S.; Thamban, M.; Sudhakar, M. Spatial distribution of diatoms in surface sediments from the Indian sector of Southern Ocean. *Curr. Sci.* **2006**, *91*, 1495–1502.
135. Medlin, L.; Priddle, J. (Eds.) *Polar Marine Diatoms*; British Antarctic Survey: Cambridge, UK, 1990.
136. Esper, O.; Gersonde, R. Quaternary surface water temperature estimations: New diatom transfer functions for the Southern Ocean. *Palaeogeogr. Palaeoclimatol. Palaeoecol.* **2014**, *414*, 1–19. [CrossRef]
137. Escutia, C.; Warnke, D.; Acton, G.D.; Barcena, A.; Burckle, L.; Canals, M.; Frazee, C.S. Sediment distribution and sedimentary processes across the Antarctic Wilkes Land margin during the Quaternary. *Deep-Sea Res. Part Ii-Top. Stud. Oceanogr.* **2003**, *50*, 1481–1508. [CrossRef]
138. Garrison, D.L.; Buck, K.R. Sea-ice algal communities in the Weddell Sea: Species composition in ice and plankton assemblages. In *Marine Biology of Polar Regions and Effects of Stress on Marine Organisms*; Gray, J.S., Christiansen, M.E., Eds.; Wiley & Jons Ltd: Chichester, UK, 1985; pp. 103–122.
139. Buffen, A.; Leventer, A.; Rubin, A.; Hutchins, T. Diatom assemblages in surface sediments of the northwestern Weddell Sea, Antarctic Peninsula. *Mar. Micropaleontol.* **2007**, *62*, 7–30. [CrossRef]
140. Taylor, F.; McMinn, A.; Franklin, D. Distribution of diatoms in surface sediments of Prydz Bay, Antarctica. *Mar. Micropaleontol.* **1997**, *32*, 209–229. [CrossRef]
141. Krebs, W.N.; Lipps, J.H.; Burckle, L.H. Ice diatom floras, Arthur Harbor, Antarctica. *Polar Biol.* **1987**, *7*, 163–171. [CrossRef]
142. Maddison, E.J.; Pike, J.; Leventer, A.; Dunbar, R.; Brachfeld, S.; Domack, E.W.; Manley, P.; McClennen, C. Post-glacial seasonal diatom record of the Mertz Glacier Polynya, East Antarctica. *Mar. Micropaleontol.* **2006**, *60*, 66–88. [CrossRef]
143. Arrigo, K.R. Sea Ice Ecosystems. *Annu. Rev. Mar. Sci.* **2014**, *6*, 439–467. [CrossRef]
144. McMinn, A.; Hodgson, D. Summer phytoplankton succession in Ellis Fjord, eastern Antarctica. *J. Plankton Res.* **1993**, *15*, 925–938. [CrossRef]
145. Rózanska, M.; Gosselin, M.; Poulin, M.; Wiktor, J.M.; Michel, C. Influence of environmental factors on the development of bottom ice protist communities during the winter–spring transition. *Mar. Ecol. -Prog. Ser.* **2009**, *386*, 43–59. [CrossRef]
146. van Leeuwe, M.A.; Tedesco, L.; Arrigo, K.R.; Assmy, P.; Campbell, K.; Meiners, K.M.; Rintala, J.-M.; Selz, V.; Thomas, D.N.; Stefels, J. Microalgal community structure and primary production in Arctic and Antarctic sea ice: A synthesis. *Elem. Sci. Anthr.* **2018**, *6*, 1–25. [CrossRef]
147. Ahn, I.Y.; Chung, H.; Kang, J.S.; Kang, S.H. Diatom composition and biomass variability in nearshore waters of Maxwell Bay, Antarctica, during the 1992/1993 austral summer. *Polar Biol.* **1997**, *17*, 123–130. [CrossRef]
148. Whitaker, T.M.; Richardson, M.G. Morphology and Chemical composition of a natural population of an ice-associated Antarctic marine diatom *Navicula glaciei*. *J. Phycol.* **1980**, *16*, 250–257. [CrossRef]
149. Scott, P.; McMinn, A.; Hosie, G. Physical parameters influencing diatom community structure in Eastern Antarctic sea-ice. *Polar Biol.* **1994**, *14*, 507–517. [CrossRef]
150. Medlin, L.; Hasle, G. Some Nitzschia and related diatom species from fast ice samples in the Arctic and Antarctic. *Polar Biol.* **1990**, *10*, 451–479. [CrossRef]
151. Fiala, M.; Kuosa, H.; Kopczynska, E.E.; Oriol, L.; Delille, D. Spatial and seasonal heterogeneity of sea ice microbial communities in the first-year ice of Terre Adelie area (Antarctica). *Aquat. Microb. Ecol.* **2006**, *43*, 95–106. [CrossRef]
152. Medlin, L. The nomenclature and type locality of *Berkeleya adeliensis* (*Bacillariophyceae*): A correction. *Plant Ecol. Evol.* **2019**, *152*, 409–411. [CrossRef]
153. Tanimura, Y.; Fukuchi, M.; Watanabe, K.; Moriwaki, K. Diatoms in Water Column and Sea-ice in Lutzhow-Holm Bay, Antarctica, and their Preservation in the Underlying Sediments. *Bull. Natl. Sci. Museum. Tokyo Ser. C* **1990**, *18*, 15–39.
154. McMinn, A.; Bleakley, N.; Steinburner, K.; Roberts, D.; Trenerry, L. Effect of permanent sea ice cover and different nutrient regimes on the phytoplankton succession of fjords of the Vestfold Hills Oasis, eastern Antarctica. *J. Plankton Res.* **2000**, *22*, 287–303. [CrossRef]
155. Fryxell, G.A. *Thalssiosira australis* Peragallo and *T. lentiginosa* (Janisch) G. Fryxell, comb. nov.: Two Antarctic diatoms (*Bacillariophyceae*). *Phycologia* **1977**, *16*, 95–104. [CrossRef]
156. Ichinomiya, M.; Nakamachi, M.; Fukuchi, M.; Taniguchi, A. Population dynamics of an ice-associated diatom, *Thalassiosira australis* Peragallo, under fast ice near Syowa Station, East Antarctica, during austral summer. *Polar Biol.* **2008**, *31*, 1051–1058. [CrossRef]
157. McMinn, A. Preliminary investigation of the contribution of fast-ice algae to the spring phytoplankton bloom in Ellis Fjord, eastern Antarctica. *Polar Biol.* **1996**, *16*, 301–307. [CrossRef]
158. Ichinomiya, M.; Gomi, Y.; Nakamachi, M.; Honda, M.; Fukuchi, M.; Taniguchi, A. Temporal variations in the abundance and sinking flux of diatoms under fast ice in summer near Syowa Station, East Antarctica. *Polar Sci.* **2008**, *2*, 33–40. [CrossRef]
159. Hasle, G.R.; Syvertsen, E.E. Chapter 2: Marine Diatoms. In *Identifying Marine Phytoplankton*; Tomas, C.R., Ed.; Academic Press: San Diego, CA, USA, 1997.

160. Leventer, A.; Armand, L.; Harwood, D.; Jordan, R.W.; Ligowski, R. (Eds.) New Approaches and Progress in the Use of Polar Marine Diatoms in Reconstructing Sea-Ice Distribution. In *Antarctica: A Keystone in a Changing World – Online Proceedings of the 10th ISAES X, Santa Barbara, CA, USA, 26 August–1 September 2007*; USGS Open-File Report 2007-1047, Extended Abstract 005, 4p; USGS: Liston, VA, USA, 2007.
161. Cremer, H.; Roberts, D.; McMinn, A.; Gore, D.; Melles, M. The Holocene Diatom Flora of Marine Bays in the Windmill Islands, East Antarctica. *Bot. Mar.* **2003**, *46*, 82–106. [CrossRef]
162. Rivera, P.; Cruces, F. Fragilaria striatula lyngbye: Una diatomea marina muy poco conocida para chile. *Gayana. Botánica* **2002**, *59*, 35–41. [CrossRef]
163. Kang, J.S.; Kang, S.H.; Lee, J.H.; Lee, S. Seasonal variation of microalgal assemblages at a s fixed station in King George Island, Antarctica, 1996. *Mar. Ecol. Prog. Ser.* **2002**, *229*, 19–32. [CrossRef]
164. Hasle, G.R.; Medlin, L.K.; Syvertsen, E.E. *Synedropsis* gen. nov., a genus of araphid diatoms associated with sea ice. *Phycologia* **1994**, *33*, 248–270. [CrossRef]
165. Cefarelli, A.O.; Ferrario, M.E.; Vernet, M. Diatoms (*Bacillariophyceae*) associated with free-drifting Antarctic icebergs: Taxonomy and distribution. *Polar Biol.* **2016**, *39*, 443–459. [CrossRef]